Chapter 10
Flute-Like Instruments

Benoît Fabre

Abstract This chapter deals with a second category of self-sustained oscillations produced by musical instruments and focuses on flutes with open ends. The following section presents the self-sustained oscillator as a looped system, focusing mostly on the jet and on its interaction with the acoustic field in the pipe. An integral approach, that allows to overpass the limitations of the looped system analysis, is also introduced. The three main elements that need to be described for modeling the oscillation in flutes are: (1) the perturbation of the jet by the acoustic field: the jet receptivity; (2) the evolution of the perturbation convected by the jet: the jet instability; and (3) the production of acoustical energy by the perturbed flow: the aeroacoustic sources. Models are proposed for each of these elements and compared to experiments. The jet-drive model is detailed and shown to be formally equivalent to the force source term in an aeroacoustic analogy. The main geometrical parameters that characterize a flute exciter is the ratio of the channel thickness to the distance between the flue exit and the labium, while the main parameter related to the instrumentalist is the jet Reynolds number.

10.1 Introduction and General Description

The first attempts to understand flute-like instruments from a physical point of view are found in the late nineteenth century, see, for example, the work by Helmholtz [48] and Rayleigh [36]. During the twentieth century, the development of fluid mechanics and more specifically studies on jet instability and aeroacoustics brought new insight on the physics of flute-like instruments.

Today's models allow producing realistic synthetic flute sounds, based on the physical description of the instrument. This indicates that the main physical mechanisms are now understood. However, this global understanding does not allow an accurate interpretation of the influence of some specific parameters, such as those

B. Fabre (✉)
Laboratoire LAM – Lutherie Acoustique Musique, and IJLRA – Institut Jean le Rond d'Alembert, Université Pierre-et-Marie-Curie, CNRS, ministère de la culture et de la communication, Paris, France
e-mail: benoit.fabre@upmc.fr

A. Chaigne, J. Kergomard, *Acoustics of Musical Instruments*, Modern Acoustics and Signal Processing, DOI 10.1007/978-1-4939-3679-3_10

of interest for players and instrument makers. This chapter focuses on open end flutes, excluding stopped pipes, and on quasi-cylindrical pipes. Indeed, the conical bore of flutes shows a behavior much closer to that of a cylinder than the bores of double reed instruments such as the oboe or the bassoon.

After a general description of the physics and of the different sound production mechanisms in flutes, the chapter will develop a general model of flutes (Sect. 10.2). We then focus on the most difficult parts, namely the description of the jet instability (Sect. 10.3) and of the aeroacoustic sources (Sect. 10.4). The main elements leading to a simplified model (Sect. 10.5) aiming at sound synthesis, will be discussed next.

10.1.1 The Air Jet, Driving the Oscillation in Flutes

The three main elements that need to be described for modeling the oscillation in flutes are

- the perturbation of the jet by the acoustic field: the jet *receptivity*,
- the evolution of the perturbation convected by the jet: the jet *instability*,
- the production of acoustical energy by the perturbed flow: the aeroacoustic *sources*.

The following section presents the self-sustained oscillator as a looped system, focusing mostly on the jet and on its interaction with the acoustic field in the pipe.

10.1.1.1 The Jet Instability

Observing the smoke emitted by a cigarette indicates that jets are naturally unstable. After a few centimeters, the thin smoke jet bends and oscillates, and finally looses its organized structure, ending as a wide cloud. This kind of (space-time) instability can be observed as soon as two fluids with different velocities are in contact. For example, the wind at the surface of the sea induces water waves. The surrounding air needs to be still in order to observe the evolution of the cigarette smoke described above: indeed, slight movements of the air around the cigarette or a movement of the hand holding the cigarette strongly influences the jet motion, demonstrating the high sensitivity of the smoke jet.

In a flute, the air jet is blown across an open end of the pipe resonator. When acoustic oscillation occurs within the resonator, the jet instability synchronizes on the acoustic oscillation, resulting in a “forced” oscillation of the jet. The hydrodynamic waves traveling on the jet have the same frequency as the acoustic oscillation. As for the oscillation described in the case of the cigarette smoke, the jet perturbation grows as it is carried by the flow, being convected downstream. In the case of a jet oscillation forced by a loudspeaker, Fig. 10.1 shows how the transverse displacement of the jet increases in the downstream direction.

Fig. 10.1 Photograph of the jet perturbation forced by loudspeakers placed at few centimeters apart from the flow, above and under it [$Re = 500$, 658 Hz, $U_j = 7.5$ m/s]. The jet is exhausting from the end of a 1 mm thick channel, seen on the *left side* of the picture

Two characteristics of the jet motion are important for the flute oscillation:

- the convection velocity of the perturbation, corresponding to the propagation velocity of the perturbation waves on the jet: to a first approximation, the convection velocity is equal to half the centerline jet velocity,
- the amplification of the perturbation, corresponding to a characteristic growth factor of the instability waves along the jet.

Both characteristics depend on frequency, but the amplification strongly depends on it: the jet instability is stronger in a frequency range depending on both the jet velocity and jet thickness. The strongest amplification appears for frequencies around $0.3\, U_j/h$, where U_j is the jet velocity and h is the thickness of the flue channel from which the jet is flowing.[1]

10.1.1.2 Acoustic Sources at the Labium of the Flute

Figure 10.2 illustrates the vocabulary used in the case of a recorder. The terminology changes according to the instrument studied: for instance, the foot of the organ pipe corresponds to the mouth of the recorder player, while the upper-lip of the mouth of the organ pipe corresponds to the labium or blowing edge of the recorder! In a transverse flute, the flue channel is created between the lips of the player.

Transverse perturbations of the jet are induced by the acoustic field. They are convected from the flue exit to the labium or blowing edge. As a result, the jet oscillates from one side to the other of the labium (Fig. 10.3). This induces a force on the labium due to the flow. This force is synchronized with the jet perturbation, and therefore with the acoustic oscillation. The reacting force of the labium acts as an acoustic source that sustains the acoustic oscillation, thus compensating for the various acoustic losses.

[1] Please note that in this chapter, we will denote the velocity as U, and the volume flow as Q, as it is of common use in fluid mechanics. This differs from the convention used in the other chapters of the book.

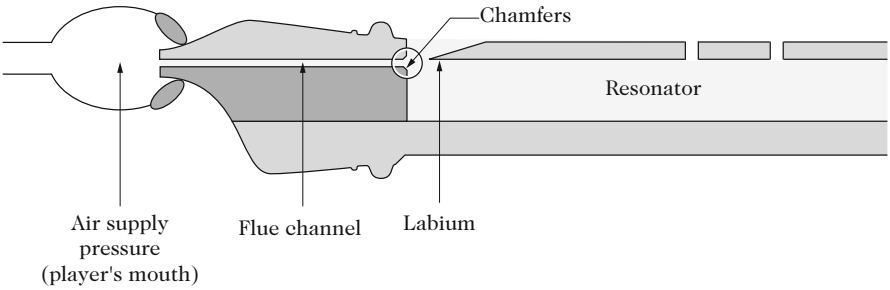

Fig. 10.2 Longitudinal sketch of a recorder, showing the terms used in this chapter. The chamfers at the flue exit can also be seen on this sketch. The opening between the flue exit and the labium is called the "mouth" in this chapter

Fig. 10.3 The acoustic field at the flue exit induces a perturbation of the jet that is amplified while it is convected towards the labium. This results into the transverse oscillation of the jet from one side of the labium to the other

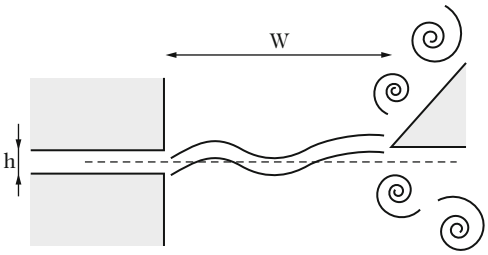

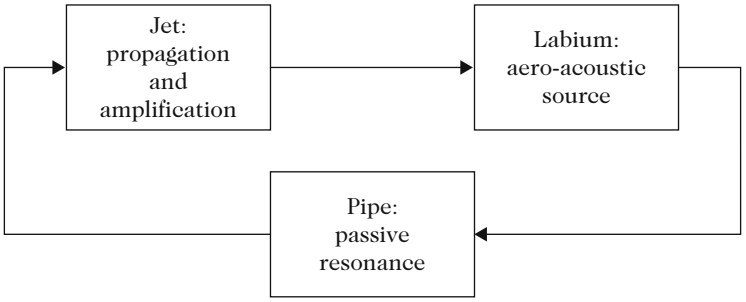

Fig. 10.4 Self-sustained oscillation in flutes can be described as a feedback loop

10.1.1.3 The Self-Sustained Oscillator as a Looped System

The acoustic field in the pipe resonator is responsible for the initial jet perturbation. This perturbation is convected and amplified downstream due to the natural jet instability. The interaction of the perturbed jet with the labium constitutes the aeroacoustic source that feeds acoustic energy into the pipe. As a response to this excitation, the acoustic energy in the pipe is associated with the acoustic flow through the mouth, that results in the jet perturbation at the flue exit. Therefore, the self-sustained oscillations in the instrument can be described as a feedback loop, as shown in Fig. 10.4.

This looped description allows to predict the oscillating frequency of the instrument. Because the pipe accumulates energy only at resonances, the oscillating frequency is close to a pipe resonance. In the looped description of the system, stationary oscillations can only occur when the total phase shift around the loop is 2π or any multiple of 2π. When blowing softly in a recorder, one can check that the time delay associated with the convection of perturbations on the jet is about half the oscillation period. The phase shift of the pipe response therefore needs to be the exact complement of one period: that is π, corresponding to another half period. If we now blow a little harder in the recorder, the jet velocity increases and the convection velocity of perturbation increases accordingly. The phase shift due to the convection of perturbations on the jet decreases and therefore the phase shift of the pipe response needs to increase: the oscillation frequency slightly increases to match the phase condition. Blowing even harder, the convection delay on the jet eventually becomes too small compared to the period of the first pipe resonance and the oscillation jumps to the second pipe resonance, for which the same convection delay represents a larger phase shift (Fig. 10.5). This is called "overblowing." For a given fingering, the player can select the oscillating regime, among the different pipe resonances, by adjusting the blowing pressure and consequently the convection jet velocity.

By blowing gently, at very low blowing pressures compared to standard playing, the player can produce very soft tones at frequencies close to the pipe resonances. This playing technique, called "whistle-tones" or sometimes "eolian tones,"

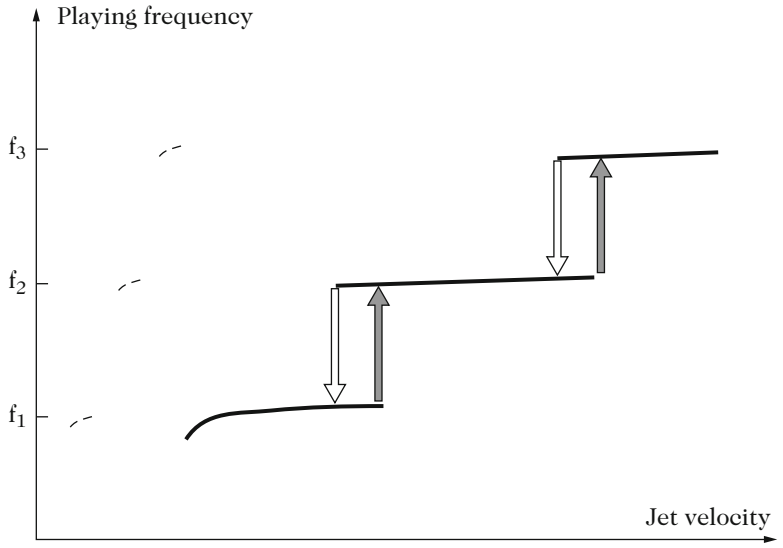

Fig. 10.5 Simplified representation of the playing frequency of a flute as function of jet velocity. The oscillation takes place at a frequency close to one of the pipe passive resonances f_1, f_2, or f_3. Regime changes do not occur at the same jet velocity for increasing (*gray arrows*) and decreasing (*white arrows*) jet velocity: a hysteresis appears. *Dotted lines* indicate whistle-tone oscillations

corresponds to convection delays on the jet that are larger than one oscillation period: one and a half or two and a half period may be observed, instead of the half period observed under standard playing conditions. These oscillations do not easily appear in recorders because of the short distance between flue exit and labium. They can appear for standard playing conditions during starting transients on some flutes and organ pipes, before the jet reaches its stationary velocity.

10.1.2 The Sounds of Flutes

10.1.2.1 The Different Elements of the Sound

Different elements are combined in the sound radiated by flutes. Using a mechanical air supply allows producing a stationary sound, as for an organ. The sound radiated by a pipe blown in such a way can be split into a deterministic part, that can be analyzed in terms of sine wave components, and a stochastic part, generated by turbulence. Indeed, turbulence produces a broadband noise, that is filtered by the pipe acoustical response. In Fig. 10.6, the FFT spectrum analysis of the stationary part of the sound of a small organ pipe shows the harmonics together with the turbulence noise filtered by the pipe. One can clearly see the shift in frequency between harmonics and pipe resonances: for example, the sixth resonance of the pipe lies between the sharp lines of the harmonics 6 and 7.

The transverse position of the labium, relative to the jet central axis, has a strong influence on the relative amplitudes of the harmonics. In the recorder, even

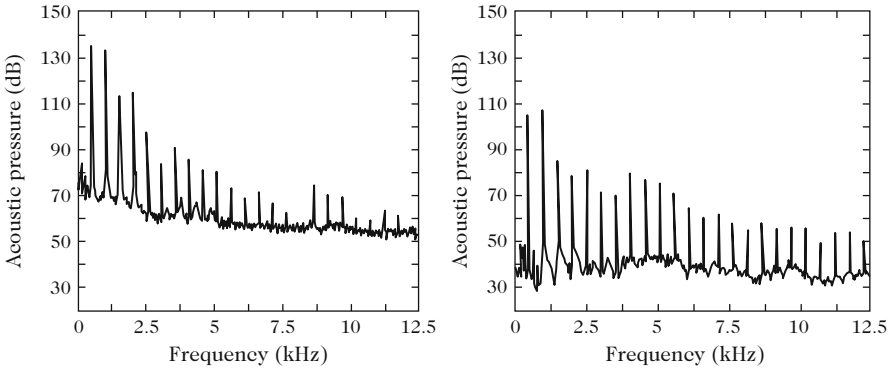

Fig. 10.6 FFT analysis of the internal pressure (*left*) and radiated pressure (*right*) at a distance of 30 cm in front of the mouth of a small organ pipe (2048 points FFT, Hanning window, averaging over 25 time slots). At frequencies higher than the fifth harmonic, (around 2.5 kHz), resonances can be identified by their filtering effect on the noise sound of turbulence, since their frequency does not coincide any more with the harmonics that correspond to the sharp peaks seen as *vertical lines* in the spectra. Radiation induces a relative amplification of the higher frequencies. From [18]

harmonics reach a minimum value for a transverse position of the labium close to the jet axis [47]. Measurements on (transverse) flute playing indicate that some players are working to enhance the amplitude of even harmonics, while some others are seeking to generate strong odd harmonics.

When the air supply comes from a player rather than from a mechanical system, pressure fluctuations modulate the sound production. Vibrato correspond to a conscious and intentional modulation of the blowing, but fluctuations are observed, even when the player aims at producing a "stable" tone. Because of these fluctuations, it is generally not possible to define a stationary part of the tone. This makes the analysis of the sound production even more difficult!

Starting transients are also quite difficult to analyze. Experiments on transients are difficult to set up, mostly because it is difficult to get an accurate and reproducible control of blowing pressure rises. Analysis is also difficult from the point of view of signal processing, while the most difficult part of the analysis of starting transients is due to the complex interaction of intricate physical phenomena [20, 46]. The different sound components, that will become the harmonics in the steady stationary part of the sound, display changing frequencies and amplitudes during the attack transient. Figure 10.7 shows the time evolution of the three first frequency components during an attack transient. In this example, the second component (with frequency close to twice that of the later fundamental) increases much faster than the first component.

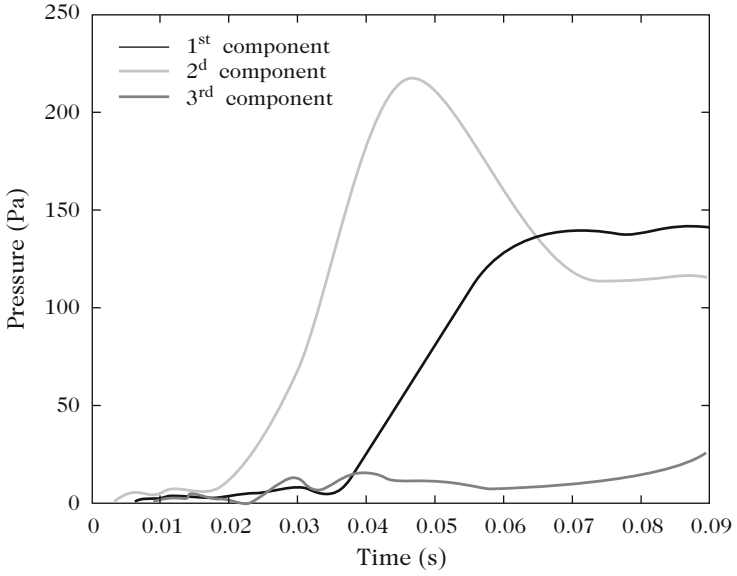

Fig. 10.7 Time evolution of the three first frequency component during the attack transient in a small organ pipe. In this case, the second component is dominating the attack transient. From [38]

10.1.2.2 Whistle-Tones or Eolian Tones

High frequency components may also appear during the attack transient [8, 20]. The frequency behavior of the so-called mouth-tones [8] shows some similarity with edge-tones. Therefore, measurements of the amplitude of these sounds (pipe internal pressure) were made under steady blowing in whistle-tone condition, showing that the amplitude is a factor 100 higher than that expected for edge-tones. Furthermore, the amplitude appears to be even higher (approximately by a factor 2) than that expected for a "normal" pipe-tone, indicating that the saturation mechanisms at work are different.

These mouth-tones, or eolian tones or whistle-tones, are relying on energy accumulation at a resonance frequency of the pipe [1]. Flute players know very well how dangerous they are because of their poor stability.

10.2 A Global Model for the Instrument

10.2.1 General Description

Before developing a physical model of a flute, the limits of the system must be clearly identified. Recall that the sound is the result of instrument–player interaction. It is therefore easier to start our description by instruments in which the player has little influence on the sound: the organ pipe, and to a lesser extend, the recorder. Both instruments have in common that the geometry of the exciter part does not change during playing, and is fully determined by the music instrument maker: jet formation channel and labium position. When the jet is blown through the lips of the player, the description is more complex because the player adapts his lip geometry during playing, in a not fully reproducible manner. A good player may aim at producing very similar sound quality when repeating a musical excerpt, but never aims at reaching the same lip geometry: the player's target is the sound, not the geometry.

Even for instruments with a fixed geometry, today's models are still very crude. They offer a good description of the physics of the instrument for a restricted range of parameters (Reynolds and Strouhal numbers, see next section). These models are only valid for specific playing techniques and fail to describe some phenomena observed during transients. Furthermore, they do not allow to include some details of the instruments such as the chamfers that are cut at the flue exit in recorders, or the nicking of some organ pipes. Direct flow simulation, solving the equations of fluid mechanics at each time step and each position in space, is still difficult nowadays when dealing with the whole instrument [31, 41], but can offer interesting answers to localized problems, providing information that can help improving simplified models [7].

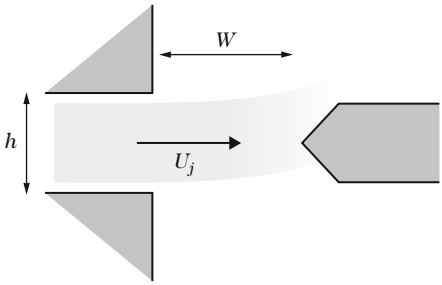

Fig. 10.8 Geometrical parameters of the exciter part. U_j is the jet central velocity at the channel exit, h is the channel thickness, and W is the flue exit to labium distance

10.2.2 Important Parameters

Oscillations in a flute can be described as the result of the coupling between a hydrodynamic mode of a jet and an acoustic mode of a pipe resonator. Different scaling parameters are useful. Figure 10.8 shows the geometrical parameters involved in this coupling.

The Reynolds number Re is used to characterize the structure of the jet: it may vary from a few hundreds (recorder) up to 10,000 in modern transverse flute playing.

$$500 < Re = \frac{U_j h}{\nu} < 10,000 \tag{10.1}$$

where U_j is the jet central velocity at the channel exit, h is the corresponding channel thickness, and ν is the kinematic viscosity of air ($\nu = 1.5 \cdot 10^{-5}$ m^2/s $= \mu/\rho$, see Sect. 5.5.2 in Chap. 5). The jet instability is characterized by the Strouhal number, corresponding to the inverse of the dimensionless frequency. Definitions of the Strouhal number may vary according to different situations and authors, from $\omega W/U_j$, with ω the angular frequency and W the flue exit to labium distance, to fh/U_j, where $f = \omega/2\pi$.

Theoretical analysis of jet instability generally uses the half-thickness parameter b of the jet, for instance, in the case of the Bickley velocity profile[2] $U(y) = U_0 \operatorname{sech}^2(y/b)$ with y the transversal coordinate [22, 34]. The relation between the experimental parameter h and the theoretical parameter b is not straightforward. To a first approximation, it can be deduced from conservation laws between the channel flow and the jet flow. For example, if the channel flow is approximated by a Poiseuille flow and the jet flow is assumed to have a Bickley velocity profile with $U_0 = U_j$, momentum conservation together with central velocity conservation lead to $b = 2h/5$ [45].

For standard blowing conditions in flutes, one half hydrodynamic wavelength λ_h can be observed on the jet between the flue exit and the labium. The wave propagation velocity on the jet is approximately equal to half the central jet velocity

[2] $\operatorname{sech} x = 1/\cosh x$

U_j, and therefore the half wavelength across the mouth width W, between flue exit and labium $W = \lambda_h/2$ corresponds to:

$$\mathrm{Str}_W = \frac{fW}{U_j} \approx 0.25 \tag{10.2}$$

which is a characteristic value in the oscillating range of the instruments [15, 21, 39, 47].

The properties of the jet instability are determined by the interaction between both shear layers, on the two sides of the jet. Therefore, the instability is often studied as function of the Strouhal number based on the transverse dimension of the jet (b or h, depending on whether the approach is theoretical or experimental): $\mathrm{Str}_h = fh/U_j$. The jet length to jet thickness ratio W/h corresponds to the ratio between the two Strouhal numbers discussed above. This ratio is an important parameter for the modeling. "Thick jets" correspond to values of this ratio smaller than 4 (in the case of transverse flute or shakuhachi, the Japanese flute, playing loud in the low register), while "thin jets" such as those found in some organ pipes are characterized by values up to 20 of the thickness ratio W/h of the jet.

Figure 10.9 shows the standard operating range of different instruments in a map representing the jet thickness W/h as function of the Reynolds number. Instruments for which the jet is formed between the lips of the player allow to vary the parameters during playing, and therefore present a wide operating range. In the case of the organ, it is the variety of pipes in the different stops that allows a wide operating range.

Models for the jet behavior need to be adapted to the specific operating range. In the organ, the same blowing system is generally used for all pipes, and the player can adjust individual blowing conditions of each pipe by varying the opening of each pipe foot. Together with different geometries of the flue and of the labium, this yields a wide operating range.

Last, the oscillating amplitude is quantified as the ratio of the acoustic velocity in the mouth of the pipe to the central jet velocity, or to the mean flow velocity of the jet. The central jet velocity is generally estimated from pressure values by applying the Bernoulli equation (see below) between the pressure reservoir and the atmospheric pressure [21, 39, 46]. The acoustic velocity in the mouth can be deduced from pressure measurement in the pipe resonator, taking the non-uniformity of the flow in the mouth [45] into account. For standard blowing conditions, oscillating amplitudes induce a transverse acoustic perturbation v_{ac} of the jet, with an amplitude V_{ac} of the order of magnitude of one-tenth of the jet velocity:

$$\frac{V_{\mathrm{ac}}}{U_j} \approx 10^{-1}. \tag{10.3}$$

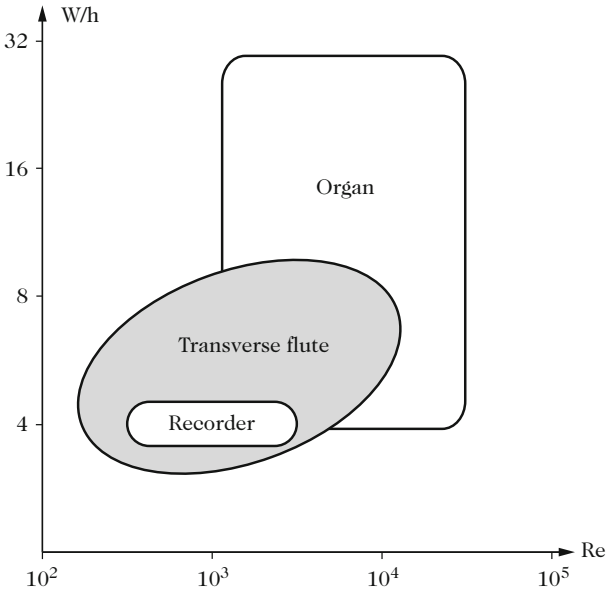

Fig. 10.9 Operating ranges of the recorder, of the transverse flute, and of the organ pipes in a map representing the jet thickness W/h as function of the Reynolds number. Transverse flute allows the player to cover a wide range on a single instrument through lip and blowing pressure adjustment, while in the case of the organ, the variety of pipes with different geometries determines the operating range

10.2.3 Localized or Distributed Interaction?

The different elements that take part in the oscillation interact in such a way that it is difficult to separate them: the acoustic resonance in the pipe cannot be separated from the radiation at the pipe ends, and the aeroacoustic source acts in the vicinity of the open end. It may seem artificial to model each element separately: the jet, the aeroacoustic sources, and the pipe resonator.

10.2.3.1 Models Assuming Localized Interaction (Lumped Models)

This separation came first from the different related scientific fields: flow instability is generally a topic of fluid mechanical studies, the pipe resonance of complex pipes is analyzed in acoustical studies, while the sound production by an unsteady flow interacting with solid boundaries is analyzed in aeroacoustical studies. Different time and space scales may allow to justify the splitting of the problem into independent problems, corresponding to different simplifications of the Navier–Stokes equation.

Jet descriptions are usually carried out under the assumption of compact flow, corresponding to small scales compared to the acoustic wavelength: the fluid is supposed to be *incompressible*[3]. In contrast, the description of the pipe acoustics usually neglects convective effects. Theses assumptions are valid, in the study of the oscillation mechanisms, only for low frequencies, corresponding to the lowest harmonics of the sound. This is justified by the fact that the oscillation mechanisms are controlled by the fundamental frequency of the oscillation, or by the two first harmonics. However, for the listener hearing the radiated sound, higher frequency components are very important. The poor radiation efficiency at low frequencies makes these two points of view compatible: low frequencies are mostly trapped inside the resonator and taking care of the self-sustained oscillation. This is because the sound waves at low frequencies are almost totally reflected at the open pipe ends, with very little radiation. The visco-thermal losses at the walls at the oscillating frequency are higher than the radiation losses. On the contrary, higher frequency components have smaller amplitudes inside the pipe, but they are much more efficiently radiated. Figure 10.6 shows the spectrum of the acoustic pressure inside the pipe, together with the spectrum of the acoustic pressure radiated at a distance of about 30 cm from the pipe mouth. Components in the frequency band from 3 to 5 kHz, corresponding to the most sensitive range of hearing, show a higher relative importance in the radiated sound than in the internal acoustic field.

10.2.3.2 Distributed Interaction Models

Lumped models with independent blocks are based on the assumption of localized interactions. The jet is supposed to be perturbed by the acoustic field at the positions of flow separation at the flue channel exit, and the sound production is supposed to be localized at the labium. The pipe resonator is then fully described by its acoustic response to this excitation at the flue exit.

A more rigorous approach can be found in analytical models, as proposed by Howe [28], Crighton [11], Elder [17], and Bechert [5]. These models describe the interaction between the flow and the acoustic field using integral formulations. These formulations can be developed for simplified geometries only, such as an infinitely thin labium, for instance, and leads to awkward mathematical developments when solving the problem. Solving is only possible under restrictive assumptions, such as infinitely thin shear layers, linear approximation of perturbations (the saturation of the oscillation is not part of the solution), or in some cases point vortices. Despite these difficulties, analytical models, together with

[3]The fluid can be considered as incompressible whenever its density ρ can be approximated to be constant. This means that the density variations induced by pressure variations can be neglected. The equation $\rho = \rho_0 =$ constant is an equation of state of the fluid, indicating that pressure changes are related to the acceleration of the fluid (Bernoulli) or to viscous forces, but not to density changes. As a consequence, one can write $\mathrm{div}(\mathbf{v}) = 0$. Of course, acoustic waves cannot be written under such an assumption. This assumption can therefore only apply within a region small compared to the acoustic wavelength, and only for flow velocities U_j that remain small compared to the velocity c of sound propagation ($M = U_j/c \ll 1$).

numerical simulation, are probably an interesting source of inspiration whenever lumped models with localized interactions fail to predict the flute's behavior. This is the reason why we will present these approaches in the following section.

10.3 A Modeling for the Jet Oscillation

The jet oscillation is described within the framework of fluid mechanics. The basic description of the flow dynamics is the same as the one used in the context of acoustics, but fluid dynamics generally focuses on different approximations. We will first discuss the jet formation at the outlet of the flue channel (in the case of a recorder) or of the lip channel (in the case of transverse flute, for example). The unstable behavior of this jet will then be addressed. The sound production associated with the interaction of the jet with the labium will be described in Sect. 10.4.

10.3.1 Jet Formation

The instrument player produces an overpressure in his mouth. As a result the air accelerates towards the low pressure area in the channel or between the player's lips. To a first approximation, our description will assume that the pressures and therefore the jet flow are constant, which correspond to stationary conditions.

10.3.1.1 The Flow in the Channel

In a frictionless approximation (inviscid flow), the circulation of the velocity round a loop is conserved (Kelvin circulation theorem). Since the circulation round a loop is related to the vorticity field, if the vorticity is zero at an initial instant, it remains zero for all subsequent times. The flow is then described as irrotational and the velocity is conservative: it is the gradient of a scalar potential $\mathbf{v} = \mathbf{grad}\,\varphi$. Starting from Euler's equation without external forces (1.101), one can write under *incompressible* assumption (mass density ρ_0 is constant, div$\mathbf{v} = 0$):

$$\rho_0 \frac{d\mathbf{v}}{dt} = -\mathbf{grad}\, p. \tag{10.4}$$

If we now assume a *stationary* flow, the time derivatives are zero. The pressure forces push the fluid into the channel in the x direction, and the velocity v_x in this direction is the only component of the flow. The previous equation then writes

$$\rho_0 v_x \frac{\partial v_x}{\partial x} = -\frac{\partial p}{\partial x}. \tag{10.5}$$

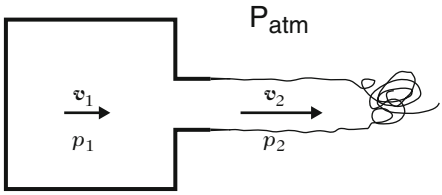

Fig. 10.10 Frictionless flow at the outlet of a pressure reservoir: application of Bernoulli's equation

The left-hand side of this equation can be written as: $\frac{1}{2}\rho_0 \partial v_x^2/\partial x$. Integrating the equation along a path from inside the pressure reservoir to a point outside in the jet yields a simplified Bernoulli equation (1.104):

$$\frac{1}{2}\rho_0(v_{x2}^2 - v_{x1}^2) = p_1 - p_2. \tag{10.6}$$

If the reservoir that accounts for the player's mouth is large enough, the integration can be carried out from a point inside the reservoir where the velocity is negligible to a point outside in the jet, where the pressure is equal to the ambient atmospheric pressure $p_2 = P_{\text{atm}}$ (Fig. 10.10). Assuming a potential flow allows this result to be independent from the path between the two considered points. A fluid particle is accelerated from the mouth (pressure higher than the atmospheric pressure, stagnant fluid, potential energy) by the pressure gradient into the flow channel down to the channel exit (atmospheric pressure and kinetic energy). The jet velocity U_j at the flue channel exit is

$$U_j = \sqrt{\frac{2\Delta p}{\rho_0}}. \tag{10.7}$$

where Δp stands for the mouth pressure relative to the atmospheric pressure: $\Delta p = p_1 - P_{\text{atm}}$.

However, this description does involve friction because of the flow separation at the channel exit. Indeed, in a strictly frictionless potential flow description, streamlines follow the walls and this would induce an infinite transverse acceleration of fluid particles at the edges of the channel exit! In an actual flow, the viscosity becomes important at this point, even if it is very small. Viscosity is responsible for flow separation and jet formation.

- *A viscous flow approach* allows describing the development of boundary layers at the channel walls. Because of viscosity, the tangential velocity is zero at the walls, and increases within a thin layer up to its nominal frictionless flow value. This transition layer is called a "boundary layer." The thickness δ of this layer grows as the flow travels downstream in the channel. The flow in the axial x direction therefore shows a transverse velocity profile $v_x(y) = U(y)$ that changes as fluid flows downstream. Friction forces due to viscosity depend on the slope

of the velocity profile $\mu(\partial U/\partial y)$, where μ is the coefficient of viscosity of the fluid. The net force on a layer of thickness dy results from viscous stresses on both sides: $\mu(\partial U/\partial y)_{y+dy}$ on one side and $-\mu(\partial U/\partial y)_y$ on the other side.

In total, the net viscous force (per unit surface $dxdz$ of the layer of thickness dy) is $\mu\partial^2 U/\partial y^2$. The momentum conservation (10.4) should take this force into consideration. Extending the viscous force in the three directions (when necessary!), leads to the Navier–Stokes equation for incompressible flows:

$$\rho_0 \frac{d\mathbf{v}}{dt} = -\mathbf{grad}\, p + \mu\nabla^2\mathbf{v}. \tag{10.8}$$

In the case of a stationary flow, this equation writes

$$\rho_0(\mathbf{v}.\mathbf{grad})(\mathbf{v}) = -\mathbf{grad}\, p + \mu\nabla^2\mathbf{v}. \tag{10.9}$$

Solving this equation in a channel is generally associated to the name of Prandtl. This is a nonlinear 2D problem. Rather than the mathematical development (see [3, 42] for reference), we now focus on its physical interpretation.

In the boundary layer along the channel walls, viscosity induces transverse transfer of momentum on a thickness that grows with time as $\delta \propto \sqrt{\nu t}$, and therefore also grows with distance x from the channel inlet. For a flow of velocity U, the boundary layer thickness can be approximated as:

$$\delta(x) \approx \sqrt{\frac{\nu x}{U}}. \tag{10.10}$$

If the channel is long enough, the two boundary layers from each side of the channel will join, resulting in the formation of a parabolic velocity profile. For a long channel of uniform thickness h, the corresponding parabolic flow velocity profile is known as the Poiseuille velocity profile[4]

$$U(y) = \frac{1}{2\mu}\frac{dp}{dx}(y^2 - h^2). \tag{10.11}$$

[4] Acoustic boundary layers discussed in Chap. 5, Sect. 5.4.2.1, are different from those studied here. In the description of the acoustic boundary layers, the linear mass acceleration $\rho_0\partial\mathbf{v}/\partial t$ takes the place of the convection term (left-hand side) in Eq. (10.9). The change between the two complementary situations is governed by the channel thickness, flow velocity, and the frequency of the acoustic phenomenon: in a cylindrical pipe, the Stokes number indicates the ratio of the pipe radius to the acoustic boundary layer thickness. The Stokes number can be seen as the combination of the Reynolds number (dimensionless flow velocity) and Strouhal number (dimensionless frequency). For a quasi-steady flow (low Strouhal) and low flow velocity (low Reynolds), the Stokes number is small and the Poiseuille velocity profile is reached, corresponding to thin pipes, also called capillaries. For high frequencies and/or wider pipes, the linear term becomes dominant and the viscous acoustic boundary layer is observed, with constant thickness as the wave travels downstream. Intermediate situations show a boundary layer that grows in space, whenever the convective term controls the development of the boundary layer.

The pressure decreases linearly with the distance x along the channel. Integrating the previous equation allows calculating the pressure gradient, as a function of the flow velocity U_0 at the channel inlet (constant velocity profile, with infinitely thin boundary layers):

$$\frac{dp}{dx} = -3\mu U_0 \frac{1}{h^2}. \tag{10.12}$$

Mass conservation between the channel inlet (uniform velocity profile) and the channel outlet yields the central velocity $U(y = 0)$ of the Poiseuille profile:

$$U(0) = 1.5U_0. \tag{10.13}$$

Before the channel exit, the flow velocity profile is determined by the time during which viscosity has smoothed the profile: for a short channel, and/or high velocity, the boundary layers are thin and the flow shows a central core with a flat velocity profile. On the opposite, a long channel, and/or a slow velocity, allows for the development of a Poiseuille-like velocity profile. In most actual applications to flute channels, the estimation of the central velocity using Bernoulli's equation (10.7) seems to be reasonable [43]. Not only the channel is relatively short, but also in the case of recorders, it is usually convergent. The decrease in channel thickness will delay the boundary layer development.

10.3.1.2 The Jet Flowing Out of the Channel

Because of viscosity, the flow separates from the walls at the channel exit in order to form a free jet.

If the end of the channel shows sharp edges, the flow separation is triggered at the edges. Indeed, a fluid particle that would stick to the walls would experience a strong localized acceleration in time and space. Even if it is low, viscosity will counteract this acceleration. This is related to the fact that edges represent singularities in a potential flow.

If the end of the channel is rounded, the flow separation point is more difficult to predict. Before the separation, the flow spreads into a divergent channel. Mass conservation indicates that the velocity in the x direction slows down as the channel gets wider. According to Bernoulli's description, this results in a rising pressure in the flow, corresponding to a change of sign of the pressure gradient in the x direction: while the pressure is decreasing in the straight part of the channel due to friction, it increases in the divergent part. The pressure in the boundary layer is equal to the pressure in the core of the flow, hence the fluid particles in the boundary layer are submitted to two opposite influences: acceleration due to viscous momentum transfer from the core of the flow to the boundary layer and deceleration due to the inverse pressure gradient. At some point in the diverging channel the balance

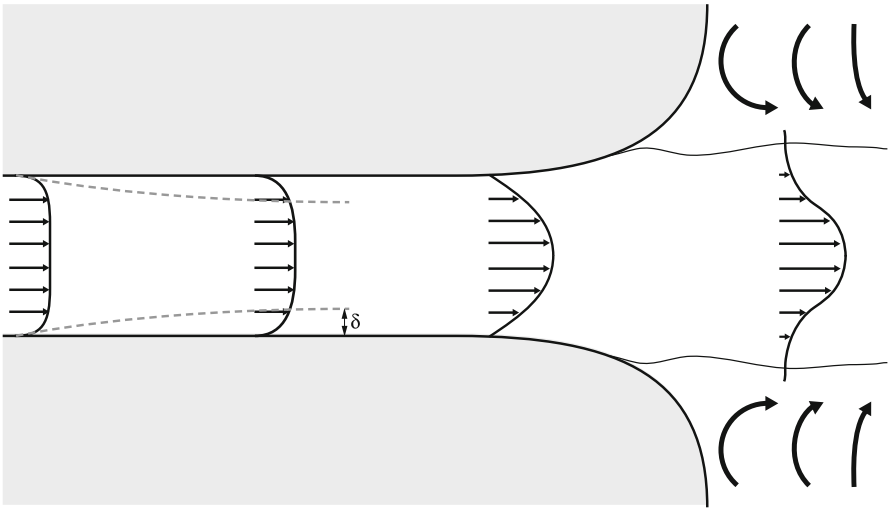

Fig. 10.11 The flow at the channel inlet has a top-hat velocity profile. As the fluid flows downstream, boundary layers get thicker because of viscosity. If the channel outlet is rounded, the flow slows down, resulting in an increase of pressure. The change of sign of the pressure gradient in the diverging part at the channel exit is responsible for flow separation. Because of viscosity, the free jet formed drags the surrounding fluid (*rounded arrows*)

between these two terms changes of sign and triggers the separation of the fluid particle at the wall, generating a stagnant fluid and/or fluid recirculation (Fig. 10.11).

In both cases (sharp or rounded edges), flow separation results in a jet that carries the memory of the channel geometry, and of upstream hydrodynamic conditions. Like a piano hammer escaping from the launching mechanism and projected against the string, the jet escapes from the control of the player. Jet characteristics such as its velocity, shape, and profile influence its behavior, like the instability that is at work in the heart of the sound production in flutes.

10.3.2 Jet Instability

An air jet flowing in air is intrinsically unstable, in the sense that any small perturbation is amplified by the jet: the example of cigarette smoke has already been discussed to illustrate this topic (see Sect. 10.1.1.1). The aim of the following section is to describe more quantitatively this instability.

10.3.2.1 Assumptions and Basic Phenomena

Assumptions

The first assumption used here is that of an inviscid fluid: as seen below, the instability of a shear flow is not driven by viscosity.[5] The second assumption is that compressibility can be ignored. This incompressibility assumption can be justified in the following cases:

- as long as the jet velocity U is kept small compared to the sound speed c,
- as long as the dimensions of the jet and sound production region are small compared to the acoustic wavelength.

Incompressibility implies a divergent free flow field div$\mathbf{v} = 0$. We will also assume for the sake of simplicity that the flow is two dimensional ($v_z = 0$). Incompressibility then writes div$\mathbf{v} = \partial v_x/\partial x + \partial v_y/\partial y = 0$. The velocity can then be written in terms of a stream function ψ:

$$v_x = \frac{\partial \psi}{\partial y} \;;\; v_y = -\frac{\partial \psi}{\partial x}. \tag{10.14}$$

Decomposition of the Velocity Field

From a general point of view, any vector field can be split into two complementary parts: a scalar potential φ part and a vector potential A part :

$$\mathbf{v} = \mathbf{grad}\,\varphi + \mathbf{curl}\,\mathbf{A}. \tag{10.15}$$

Of course, the acoustic field is part of the first contribution $\mathbf{grad}\,\varphi$ because it involves compressibility ($\nabla.\mathbf{v} = \nabla^2\varphi$). The second contribution takes into account the rotational part of the flow:

$$\boldsymbol{\omega} = \mathbf{curl}\,\mathbf{v} = \mathbf{curl}(\mathbf{curl}\,\mathbf{A}).$$

The following description is based on the evolution of the vorticity $\boldsymbol{\omega}$. This evolution can be studied by calculating the curl of the equation of motion (10.4):

$$\mathbf{curl}\left(\rho\frac{d\mathbf{v}}{dt}\right) = -\mathbf{curl}\,\mathbf{grad}\,p, \quad \text{therefore} \quad \frac{d\boldsymbol{\omega}}{dt} = 0. \tag{10.16}$$

This shows that in a frictionless flow, vorticity is conserved by the fluid particles: vorticity is convected at the local fluid velocity. In a two dimensional flow, a point

[5] Even if viscosity may be responsible for the formation of the sheared flow.

vortex of circulation Γ ($\Gamma = \oint_C v.d\ell$ on any contour C around the vortex) induces a tangential velocity field with amplitude decreasing away from the vortex. Symmetry of the flow around a point vortex allows calculating this tangential velocity v_θ induced by the vortex at a distance r from the vortex core:

$$v_\theta = \frac{\Gamma}{2\pi r}. \tag{10.17}$$

This corresponds to the Biot–Savart induction law. The instability of a shear layer can most efficiently be described starting from the flow induced by vorticity.

Kelvin–Helmholtz Instability Mechanism

Let us start the physical analysis of the jet instability with a simple case: the flow at the planar interface between two areas of the fluid with different velocities. This is known as the Kelvin–Helmholtz instability [16, 42]. This flow can be described by the relative velocity U between the two areas (see Fig. 10.12):

- $v_x = U/2$ if $y > 0$
- $v_x = -U/2$ if $y < 0$
- $v_y = 0$.

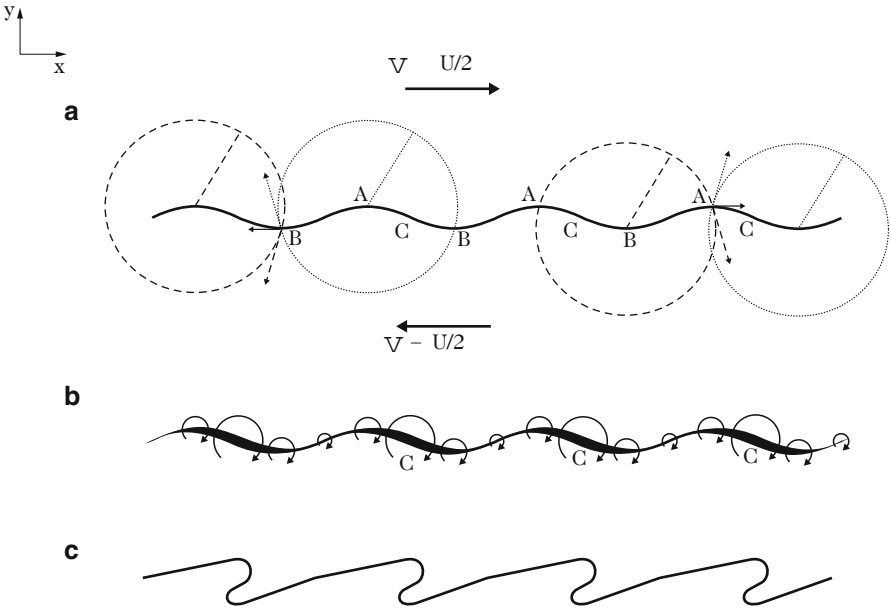

Fig. 10.12 The instability mechanism of a perturbed shear layer: (**a**) a perturbation of the interface induces local convection that concentrates (**b**) the vorticity at points C. This concentration amplifies the initial perturbation, leading to the formation of rolled structures (**c**)

The ***curl*** of the velocity field, $\boldsymbol{\omega}$, is zero everywhere except for $y = 0$: the interface is a line of vorticity. The three components of the ***curl*** are:

- $\omega_x = 0$
- $\omega_y = 0$
- $\omega_z = \partial v_y/\partial x - \partial v_x/\partial y = -\partial v_x/\partial y$.

As long as the interface remains unperturbed, the velocity field induced by the vorticity vanishes everywhere. Indeed, the transverse contributions to the velocity field at one given point of the interface due to the left side are fully compensated by the contributions on the right side. If we now assume the interface to be perturbed by a sinusoidal transverse motion, contributions from left and right sides to the local motion are no longer symmetrical. Figure 10.12 shows how this asymmetry induces a convection of vorticity of the upper parts (A) of the perturbed interface towards the right, while the lower parts (B) are convected towards the left. As a result, vorticity concentrates at the zero decreasing positions (C) of the interface.

This vorticity accumulation induces asymmetrical velocities, that contribute to the amplification of the initial perturbation, up to the point where waves break (Fig. 10.13).

10.3.2.2 Instability of an Infinite Jet

Rayleigh's Theory of an Infinite Jet

A jet can be described as two shear layers interacting with each other. The instability of an infinite jet has first been analyzed by Rayleigh [36]. The unperturbed jet in the x direction is given by:

Fig. 10.13 Wavy clouds in Wyoming, USA are induced by different wind velocities in neighboring layers (photo B.E. Martner, NOAA Environmental Technology Laboratory, Boulder)

- $v_x = U(y)$
- $v_y = 0$.

where $U(y)$ is the velocity profile of the jet. It satisfies the boundary conditions $U(\infty) = U(-\infty) = 0$ and we will further assume that the velocity profile has a single maximum. The curl of the velocity is

- $\omega_x = 0$
- $\omega_y = 0$
- $\omega_z = -\partial U(y)/\partial y = \Omega_z$.

The perturbed flow then writes

- $v_x = U + v'_x$
- $v_y = v'_y$
- $\omega_z = \Omega_z + \omega'_z$.

The vorticity conservation $d\boldsymbol{\omega}/dt = 0$ is

$$\frac{\partial(\Omega_z + \omega'_z)}{\partial t} + (U + v'_x)\frac{\partial(\Omega_z + \omega'_z)}{\partial x} + v'_y\frac{\partial(\Omega_z + \omega'_z)}{\partial y} = 0. \tag{10.18}$$

Because Ω is the steady unperturbed vorticity, it does not change in time nor in space and $\partial\Omega_z/\partial t = 0$ and $\partial\Omega_z/\partial x = 0$. For small enough perturbations, a linear approximation can be used. Products of perturbation terms are then neglected, and the previous equation becomes

$$\left(\frac{\partial}{\partial t} + U\frac{\partial}{\partial x}\right)\omega'_z + v'_y\frac{\partial\Omega_z}{\partial y} = 0 \tag{10.19}$$

where the last term shows the dependence of the jet on the second derivative of the velocity profile $\partial^2 U(y)/\partial y^2$. We now look for harmonic and propagative solutions[6] $\exp(j\omega t)\exp(-j\alpha x)$. Using $\omega'_z = \partial v'_y/\partial x - \partial v'_x/\partial y$, and the incompressibility condition $\partial v'_x/\partial x + \partial v'_y/\partial y = 0$ the previous equation turns into Rayleigh's equation:

$$\left(U(y) - \frac{\omega}{\alpha}\right)\left(\frac{\partial^2 v'_y}{\partial y^2} - \alpha^2 v'_y\right) - v'_y\frac{\partial^2 U(y)}{\partial y^2} = 0. \tag{10.20}$$

The transverse component of the perturbation v'_y is obtained by solving this equation. One needs the help of the stream function ψ' of the perturbation to calculate the longitudinal component of the perturbation. The stream function has the same harmonic propagative form $\psi'(x, y, t) = \Psi'(y)\exp(j\omega t)\exp(-j\alpha x)$.

[6]Notice that ω is the time periodicity (angular frequency) of the perturbation, while $\boldsymbol{\omega} = (0, 0, \omega_z)$ is the curl of the velocity.

All perturbation terms can be calculated from the stream function function amplitude Ψ', solution of:

$$\left(U(y) - \frac{\omega}{\alpha}\right)\left(\frac{\partial^2 \Psi'}{\partial y^2} - \alpha^2 \Psi'\right) - \Psi' \frac{\partial^2 U(y)}{\partial y^2} = 0. \tag{10.21}$$

Spatial Versus Temporal Analysis

When the jet velocity profile $U(y)$ is known, a dispersion relation is obtained, linking the time and space periodicity ω and α of the solution, by assuming boundary values $\Psi'(y) \rightarrow 0$ far from the jet ($y \rightarrow \pm\infty$). Depending on the problem studied, two resolutions can be carried out:

- the space dependence ($\alpha = \alpha_r + j\alpha_i$) of the perturbation with fixed time periodicity (ω real). Such a perturbation grows with distance as $\exp(\alpha_i x)$ with a phase velocity associated to the convection of the perturbation $c_p = \omega/\alpha_r$. A hydrodynamic wavelength $\lambda_h = 2\pi c_p/\omega = 2\pi/\alpha_r$ results from this propagation. This is a spatial analysis.
- the time dependence (ω then being complex) that results from a perturbation with specific real wavenumber α_r, corresponding to imposed geometry conditions. The perturbation then grows or vanishes in time, according to the sign of α_i. This is a temporal analysis.

The oscillating frequency in flutes is strongly dependent on the acoustic resonances of the pipe. Therefore, a spatial analysis is generally preferred.

Sinuous and Varicose Modes

If the jet velocity profile is symmetrical about $y = 0$, perturbations on both shear layers of the jet can be symmetrical or anti-symmetrical, depending on the symmetry properties of the initial perturbation of the jet. Symmetrical perturbations induce the so-called varicose oscillations of the jet, associated with a modulation of the jet thickness (see Fig. 10.14). Anti-symmetrical perturbations correspond to "sinuous" oscillations of the jet. Solving Rayleigh's equation (10.21) indicates that sinuous oscillations have a stronger amplification than varicose oscillations.

Furthermore, jet visualizations in various flute configurations indicate that the sinuous motion dominates under standard blowing conditions. In some cases, varicose contribution can be observed, which has an influence on the spectral content of the sound.

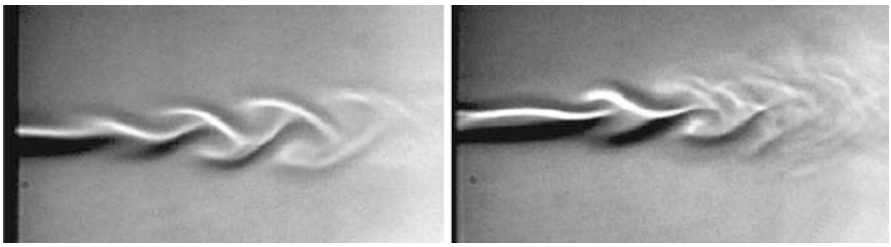

Fig. 10.14 Flow visualization of a jet submitted to an acoustic perturbation: following the initial jet perturbation, sinuous motion can be dominant (*left*) or varicose can be dominant (*right*)

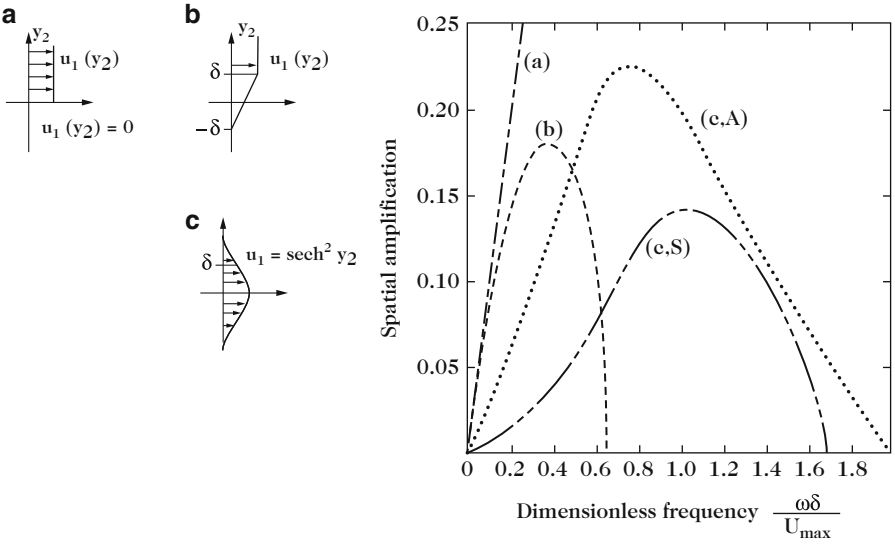

Fig. 10.15 Spatial amplification on a shear layer for different velocity profiles. (**a**), (**b**), and (**c**): simple shear layers, after Blake [6]. The amplification corresponds to anti-symmetrical jet oscillations [sinuous: (c,A)] or symmetrical [varicose: (c,S)]. Note that sinuous oscillations are better amplified than varicose oscillations

Solutions of the Rayleigh Equation

Depending on the jet velocity profile $U(y)$, Eq. (10.21) can be solved either analytically or numerically. In the case of a spatial analysis, Fig. 10.15 shows the frequency dependence of the spatial growth of perturbations on the jet. The dimensionless amplification coefficient $\alpha_i\delta$ uses the shear layer thickness δ as the spatial scale of the problem. The dimensionless frequency is the Strouhal number $\mathrm{Str}_\delta = \omega\delta/U_{\max}$, where $U_{\max}$ is the maximal value in the jet velocity profile.

It can be checked that, in the case of an infinitely thin shear layer such as the one discussed above (Kelvin–Helmholtz), the amplification increases monotonously with frequency, as already mentioned by Rayleigh. Such a thin shear layer is purely

theoretical since viscosity, even if it is very low, spreads the shear layer. All other velocity profiles with finite shear layer thickness show a maximum of amplification and then fall down below zero for Strouhal number of the order of unity. As a matter of fact, the jet does not amplify the perturbation anymore when the hydrodynamic wavelength $\lambda_h = 2\pi c_p/\omega$ gets smaller than the shear layer thickness δ.

10.3.2.3 Receptivity and Jet Oscillation in a Flute

The Jet Motion

Rayleigh's theory, presented above, is based on an infinite parallel jet flow assumption. In flutes, the jet is formed at the flue exit and flows through a window where strong transverse acoustic flows can be experienced, due to the accumulation of acoustical energy in the pipe resonator. A first step in this direction is to consider a semi-infinite jet, with negligible transverse displacement at the flue exit.

The transverse displacement $\eta(x,t)$ of the jet in the y direction can be calculated by integration of the transverse velocity from the flue exit to the actual position x. This transverse velocity is made of two components: the perturbation term v'_y exponentially growing with the distance from the flue exit, and the air displacement due to the acoustic velocity $v_{\rm ac}$:

$$\eta(x,t) = \int_{t-x/U_0}^{t} \left[v'_y(x',t') + v_{\rm ac}(x',t')\right] dt', \tag{10.22}$$

if $x' = x - (t-t')U_0$.

For long enough distances from the flue exit, one can ignore the contribution of the acoustical displacement. The transverse jet displacement then writes[7]

$$\eta(x,t) \approx -\int_{t-x/U_0}^{t} \frac{\partial \psi'(x',t')}{\partial x} dt'. \tag{10.23}$$

This implies a growth of the amplitude of the jet displacement η with $\exp(-\alpha x)$

Receptivity: The Jet Initial Perturbation

The sinuous jet motion comes from the anti-symmetrical perturbation by the acoustic field. The way the acoustic field produces the initial jet perturbation is called the *receptivity*. To a first approximation, we will assume that the initial perturbation is localized at the flue exit. In an incompressible inviscid flow approximation, this can

[7] Indeed $v'_y = -\partial\psi'(x',t')/\partial x$, which may be the reason why some authors make a confusion between the jet transverse displacement η and the stream function ψ' of the perturbation.

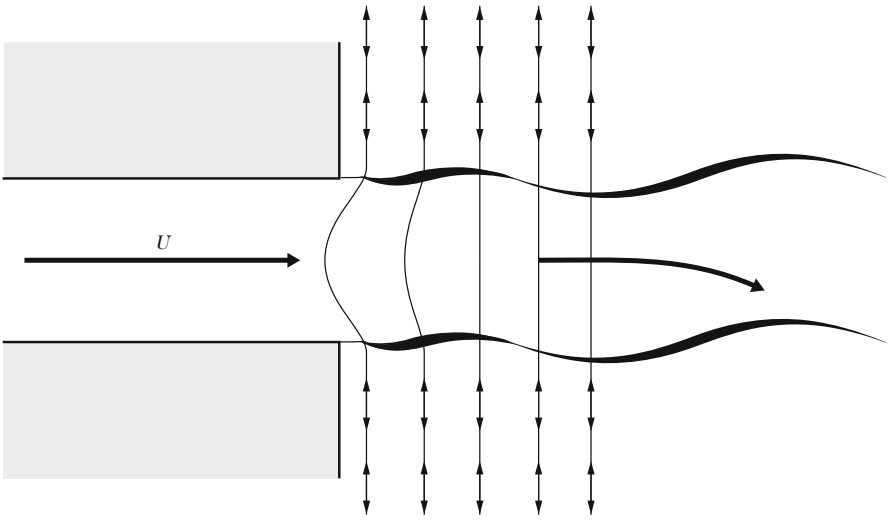

Fig. 10.16 The initial jet perturbation by the acoustic field is localized at the flow separation points where the jet is formed

be justified by the vorticity conservation in the flow. The jet perturbation can be represented as a modulation of the vorticity in the flow. Because of the vorticity conservation, such a vorticity modulation can only be injected at the separation points of the flow, due to local viscous effects. The amplification that occurs downstream is only a consequence of the jet instability, in terms of redistribution of the initial vorticity (Fig. 10.16).

Details of the geometry and of the flow in the vicinity of the flow separation points can strongly affect the receptivity [7]: boundary layer thickness in the channel just upstream from the flue exit and the geometry of the channel exit are of great influence. This is in line with the observation of recorder makers who give great care to the cutting of chamfers at the end the channel, as well as with the transverse flute players' claim that small irregularities on the player's lips strongly affect the tone quality.

Receptivity: An Empirical Model

A simplified description of the jet oscillation is generally considered for the global analysis of the oscillation in flutes. The description integrates some of the results of the analysis presented and, in particular, the exponential spatial growth α_i of the perturbation together with the convection of the perturbation. In the case of a harmonic perturbation, the transverse jet displacement η at a distance x from the flue exit is written as:

$$\eta(x,t) \approx \eta_0 e^{\alpha_i x} e^{j\omega(t-x/c_p)}. \tag{10.24}$$

Even if this description cannot fulfill the initial condition $\eta(0,t) = 0$, it offers a fairly good approximation of the jet displacement for distances from the flue exit larger than the channel thickness ($x \geq h$), provided that the initial value η_0 is correctly chosen. The perturbation being triggered by the acoustic velocity, the initial jet displacement is expected to be proportional to V_{ac}/U_j and h:

$$\eta_0 \approx \frac{V_{\mathrm{ac}} h}{U_j}. \tag{10.25}$$

Experimental data [14] indicate that the receptivity of the jet can be interpreted in terms of the relative thickness of shear layers in the jet $\delta_j = L/\sqrt{Re}$, where L is the flue channel length, and acoustic boundary layers $\delta_{\mathrm{ac}} = \sqrt{2\nu/\omega}$ as follows:

$$\eta_0 = \frac{V_{\mathrm{ac}} h \delta_j}{U_j \delta_{\mathrm{ac}}}. \tag{10.26}$$

This approach allows the dependence of the receptivity on both the frequency and jet velocity to be introduced. More recent studies by Blanc [7] indicate that the effect of chamfers found in recorders can be split into two complementary contributions: a protection effect reducing the effective V_{ac}/U_j due to the standing back of the flow separation points and an orientation of the perturbative acoustic velocity, locally following the wall geometry.

The Upper Limit of the Linear Analysis: Jet Roll Up and Vortex Formation

Rayleigh's description of the evolution of a perturbation on the jet uses a linearization of the equations [see Eq. (10.19)]. From a physical point of view, the accumulation of the shear layers' vorticity at the inflexion points in the shear layer is responsible for the growth of the perturbation. For transverse jet displacement of the same order of magnitude as the jet thickness, the jet appears to roll up and break down into discrete vortices.

The flow can then be described as an alternate vortex street, as described by Von Kármán. In order to be stable, the vortex street needs to follow the correct relation between the hydrodynamic wavelength λ_h, the street width b, the circulation Γ of vortices, and the convection velocity c_{Vx} of the street:

$$c_{Vx} = \frac{\Gamma \pi}{\lambda_h} \tanh\left(\frac{\pi b}{\lambda_h}\right). \tag{10.27}$$

Experiments show that the amplitude of the transverse jet displacement for which the linear behavior (exponential growth) turns into a vortex street is close to the jet thickness. However, this amplitude does not depend on the distance between the flue exit and the transition point, while this distance depends on the perturbation amplitude (see Fig. 10.17).

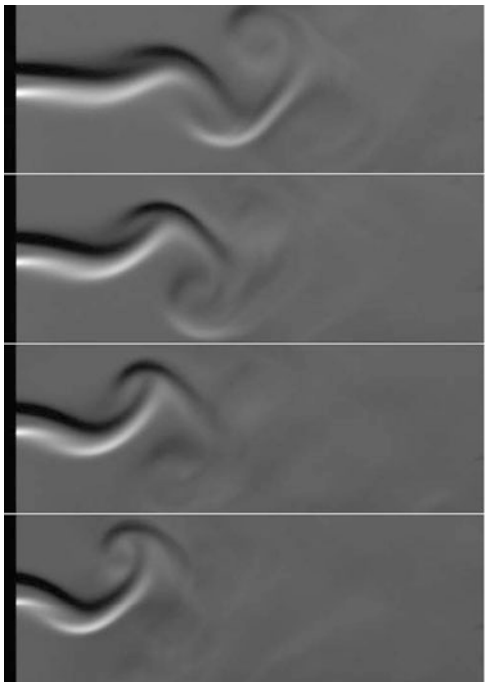

Fig. 10.17 Visualization of a jet submitted to a transverse acoustic field. From *bottom* to *top*, the excitation amplitude V_{ac} grows from 0.5 to 6.5 % of the jet velocity U_j. The jet transverse displacement grows linearly, up to the point where the jet breaks down into a row of alternate vortices, forming a vortex street. The formation of the vortex street occurs closer to the flue exit when the excitation amplitude is increased. From [14]

10.3.3 Turbulent Jet

As the jet velocity increases, its structure becomes chaotic. For values higher than a threshold, the jet is disorganized and spreads rapidly with distance. This chaotic behavior is called turbulence. This threshold depends on the geometry of the jet as well as on the fluid viscosity. It is expressed in terms of the Reynolds number $Re = U_j h/\nu$, where h is the jet channel thickness, and ν is the kinematic viscosity of air. While turbulence always develops sooner or later on the jet (see Fig. 10.18), for values of the Reynolds number smaller than 2000, the jet remains laminar for a short distance. For values above 3000, the jet becomes turbulent immediately downstream the flue exit. Estimations under playing conditions for different recorders indicate that the Reynolds number varies between 700 and 2000.

In order to produce loud sounds with flutes, the instrument and the blowing technique must allow to blow hard, that is to blow large air flows. Therefore, in most of the flutes intended for outdoor playing, one finds high values of the Reynolds number, sometimes higher than 10^4. The jet then becomes rapidly turbulent and the above description of the jet instability becomes inaccurate.

Several aspects are to be considered in this case:

- a strong decrease of the jet velocity with distance,
- a strong spreading of the jet,
- kinetic energy dissipation.

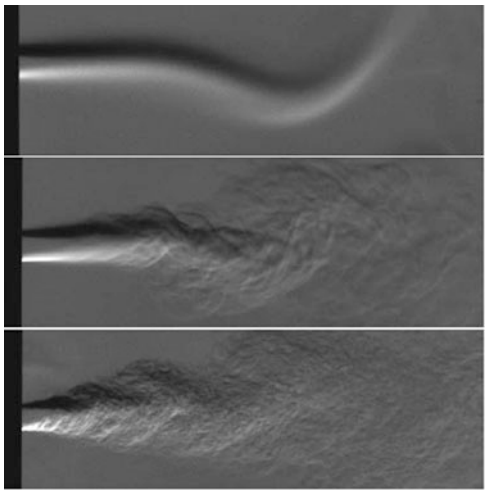

Fig. 10.18 Jet perturbed by an acoustic field. The Reynolds number in the jet increases from 200 (*top*) to 500 (*middle*) up to 3000 (*bottom*). The jet remains laminar all along the observation window for $Re = 200$. On the opposite, turbulence develops rapidly downstream of the flue exit for $Re = 3000$

A consequence of the turbulent structure of the jet is a wideband noise production. This is well known in the case of traditional instruments for outdoor music, for which a loud sound is required. The associated strong wideband noise is a part of the sounding aesthetics of these instruments. In the case of the modern Boehm flute, the quest for a "pure" tone in the sounding aesthetics of the instrument at the beginning of the twentieth century, until 1935, is challenging for the player since he has to handle a tricky compromise between sound power and tone purity (Fig. 10.19).

10.4 Aeroacoustic Sound Sources

The interaction of the oscillating jet with the labium produces the acoustic energy that sustains the oscillation in the resonator. The largest jet oscillation takes place at a position where the resonator shows a strong reaction: the labium is an edge at an open pipe end, where the acoustic velocity is maximum. Furthermore, a sharp labium induces a local singularity in the acoustic field. The same jet oscillation in free field or at less reactive position in the resonator would not produce as much sound.

Helmholtz was the first to describe the sound production by the end of the nineteenth century. In the first edition of his book [48], the jet oscillation is described as injecting fluid in the pipe at each period of the oscillation. Rayleigh argued to Helmholtz that the labium is at an open end of the pipe, where acoustic pressure fluctuations p_a are small. The mechanical work associated to volume flow injection Q is therefore weak:

$$W = \int_T p_a Q dt. \tag{10.28}$$

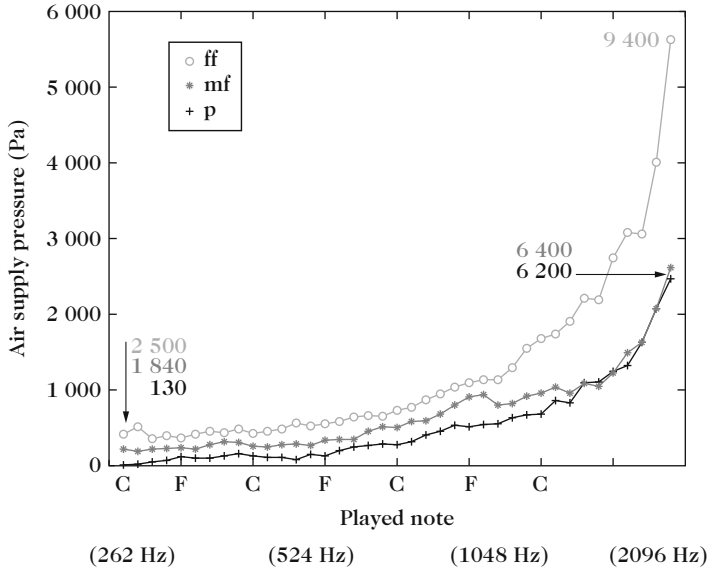

Fig. 10.19 Mouth pressure in modern Boehm flute playing as function of the pitch, for three different dynamics: *plus symbol*, *p*; *filled circle*, *mf*; *open circle*, *ff*. Estimated values of the Reynolds number are added on the plot

Conversely, the acoustic velocity is maximum at the open pipe end, therefore Rayleigh suggests that the acoustic source is a force F_a acting on the acoustic field. Such a source is more efficient since the work is then proportional to the local acoustic velocity v_a:

$$W = \int_T F_a v_a dt. \tag{10.29}$$

However, Rayleigh does not give any clue on the physical origin of this force. Several mechanisms may contribute to this force, such as the jet oscillation and the turbulence. Estimations of the acoustical power produced shows an order of magnitude of 10 mW [20].

10.4.1 The Jet-Drive Model

This model is based on Helmholtz's description: indeed, he modified his text in the second edition, taking Rayleigh's arguments into consideration! Developing Helmholtz's idea, the model takes the two flow injections on both sides of the labium into account. The two sources Q_{in} and Q_{out}, placed a small distance δ_d from each other, have fluctuating parts Q_1 and Q_2 with opposite phases ($Q_1 = -Q_2$). Therefore, they generate a pressure difference (see Fig. 10.20).

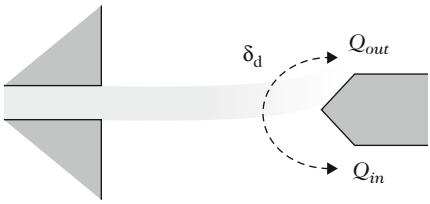

Fig. 10.20 The jet oscillation can be described as two flow injections on both sides of the labium. The fluctuating parts of the two volume flows show opposite phases $Q_1 = -Q_2$, at a short distance δ_d. In a low frequency approximation, the two sources are separated by a short distance in a small pipe. It can be represented by an equivalent pressure difference given in Eq. (10.30)

The model is developed in a low frequency approximation. Plane waves propagate in the resonator, which is therefore represented as a 1D transmission line. Assuming that the source dimensions are small compared to the acoustic wavelength, the resonator is described as a main pipe and a short thinner pipe since the open end in the mouthpiece always has a smaller cross-section area than the pipe. In this 1D representation, the two sources with opposite phases Q_1 and Q_2 are placed in the thin short pipe, at a short distance δ_d from each other (see Fig. 10.21). They constitute a dipole confined in the small pipe of cross section S_m, and produce an alternate motion of the air mass $\rho\delta_d S_m$ between the two sources.[8] The acceleration of this air mass generates the force acting on the acoustic field. This force can be written in terms of a pressure difference acting across the mouth of the pipe:

$$\Delta p = -\frac{\rho}{S_m}\delta_d \frac{d}{dt} Q_1, \tag{10.30}$$

that the source maintains between both sides of the labium. Therefore, the source can be seen as a localized pressure step across the mouth, even if both volume flow injection points are at a small distance.[9]

[8] Please note that the initial model by Helmholtz took only the inner volume flow injection into account, leaving the outer volume flow injection Q_{out} aside. However, even if the outer volume flow injection appears to be outside the pipe from a geometrical point of view, it definitely is inside the instrument from the acoustic point of view, since the limit between inner and outer field is not clearly defined from the acoustic point of view, that is within the scale of the acoustic wavelength.

[9] In Chap. 1, sources in a pipe have been discussed, using Eqs. (1.134) and (1.135). The source term in (1.134) can be written as:

$$-\frac{\rho}{S_m}\frac{d}{dt}\left[Q_1\delta(x-x_1) + Q_2\delta(x-x_2)\right] = -\frac{\rho}{S_m}\frac{d}{dt}Q_1\delta_d\frac{d}{dx}\delta(x-x_1).$$

The second expression uses the Taylor development at x_1, since $x_2 = x_1 - \delta_d$ and $Q_1 = -Q_2$. Equation (1.135) gives the equivalent force:

$$f = -\rho\frac{d}{dt}Q_1\delta_d.$$

this force balances the pressure difference $f = S_m(p_1 - p_2) = S_m\Delta p$, and corresponds to (10.30).

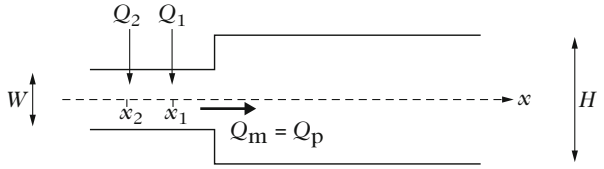

Fig. 10.21 Simplified model of a flute. Injection of two volume flows sources is equivalent to a pressure step, in a l ow frequency approximation. W and H are the flue exit to labium distance and the pipe height: in a 2D geometry, they are proportional to the areas S_m and S of mouth and pipe, respectively. The distance between the sources is $x_1 - x_2 = \delta_d$. The flow rates Q_m and Q_p through mouth and in the pipe, (that are used in the simplified model in Sect. 10.5.4) are equal since the pressure difference source *does not affect the flow rates*

The distance δ_d corresponds to the distance between the injection points Q_1 and Q_2: it corresponds to the distance associated with the potential difference in a potential theory. It can be calculated from the estimated injection positions, using conformal mapping for idealized geometries [35] (see also Chap. 7, Sect. 7.6.3.2).

10.4.2 A Discrete Vortex Model

As discussed earlier in this chapter, the jet oscillation results from the perturbation of the vorticity in the shear layers: the velocity field can be described as a potential flow on top of which two films of vorticity are added, which are modulated at the flue exit by the acoustic perturbation. The transverse motion of the jet results from the progressive concentration of vorticity at specific points, and the jet can therefore be described as a succession of line vortices shifted between the two shear layers. In such as description, the sound production can be seen as the work performed on the acoustic field by the Coriolis force associated with the convection of vortices. The force per unit volume f generated by a vortex of vorticity $\boldsymbol{\omega}$ and moving at the local fluid velocity $\boldsymbol{v}$ is given by:

$$\mathbf{f} = -\rho_0(\boldsymbol{\omega} \wedge \boldsymbol{v}). \tag{10.31}$$

The acoustic power produced per unit volume is the scalar product $\mathbf{f}.\mathbf{v}_{\text{ac}}$, where $\mathbf{v}_{\text{ac}}$ is the acoustic velocity. In this approach, the velocity field $\mathbf{v}$ is split into two contributions: the potential and the rotational components [see Eq. (10.15)]. The acoustic velocity then corresponds to the fluctuating part of the potential component of the field:

$$\mathbf{v}_{\text{ac}} = \mathbf{grad}\varphi - \langle \mathbf{grad}\varphi \rangle. \tag{10.32}$$

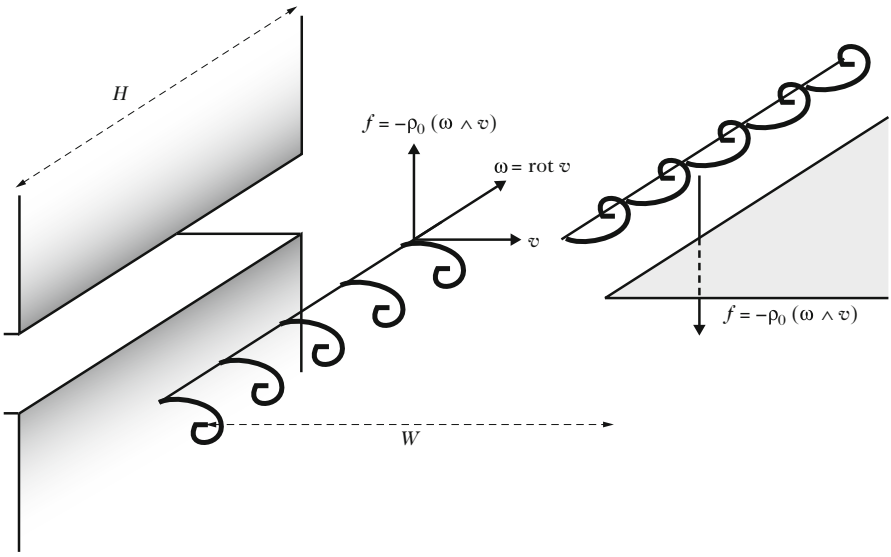

Fig. 10.22 The sound production is represented as the work performed on the acoustic field by the Coriolis force associated with the convection of vortices

where the brackets $\langle x \rangle$ indicate the time average of x. The acoustic power produced becomes

$$P_{\text{vortex}} = \frac{1}{T} \int_T \int_{\text{vol}} -\rho_0 (\boldsymbol{\omega} \wedge \boldsymbol{v}).\mathbf{v}_{\text{ac}} dV dt, \tag{10.33}$$

where vol is the volume where the source term $(\boldsymbol{\omega} \wedge \boldsymbol{v}).\mathbf{v}_{\text{ac}}$ is not vanishing (Fig. 10.22).

Sound production is restricted to areas where the force is parallel to the acoustic field, which of course corresponds to a condition for accelerating the acoustic motion. This is why the sound production is dominated by the vortex line the closest to the labium edge: indeed, the acoustic velocity is maximum around the labium edge because of the singularity associated with a sharp edge in a potential flow. Estimation of the sound power in the case of edge-tones [26] as well as in the case of flutes [15] shows that the sound production can be reasonably estimated taking only the vortex line closest to the edge into account. This explains why the sound quality is very sensitive to the shape of the edge of the labium. Vortices carried further downstream into the pipe have a velocity $\boldsymbol{v}$ parallel to the acoustic velocity $\mathbf{v}_{\text{ac}}$ so that the source term $(\boldsymbol{\omega} \wedge \boldsymbol{v}).\mathbf{v}_{\text{ac}}$ vanishes.

10.4.3 Aeroacoustic Formulation

The modeling of the acoustic source presented in the previous sections is based on the assumption that the source mechanism is localized in the vicinity of the labium edge. In a complementary approach, sound production can be described through an integral description. Several frameworks can be found, called aeroacoustic analogies: the one that is behind the description using discrete vortex lines presented above is basically the description used by Howe [28]. The following section presents the approach by Lighthill (see, for example, [12, 23, 25, 37]).

10.4.3.1 Lighthill's Analogy

In the analogy of Lighthill, one assumes a spatially limited region of sound production by the flow. The sound generated propagates to an observer located outside the source region, in a stagnant uniform fluid of density ρ_0 and sound velocity c_0. The flow at the observer's position is assumed to be described by the acoustic approximation.

Lighthill's analogy is obtained by rewriting the basic equations of flow motion. It is based on the time derivative of the mass conservation[10]:

$$\frac{\partial}{\partial t}\left[\frac{\partial \rho}{\partial t}+\frac{\partial \rho v_i}{\partial x_i}\right]=0, \tag{10.34}$$

and on the divergence of the momentum conservation equation:

$$\frac{\partial}{\partial x_i}\left[\frac{\partial \rho v_i}{\partial t}+\frac{\partial \rho v_i v_j}{\partial x_j}\right]=-\frac{\partial}{\partial x_i}\left[\frac{\partial P_{ij}}{\partial x_j}\right], \tag{10.35}$$

where P_{ij} is the stress tensor, due to pressure p and viscous stresses τ_{ij} ($P_{ij} = p\delta_{ij} - \tau_{ij}$).[11]

The fluid density ρ is split into its mean value ρ_0 at the observer's position and fluctuating component $\rho = \rho_0 + \rho'$ with $\partial^2\rho/\partial t^2 = \partial^2\rho'/\partial t^2$. Subtracting the two equations above and subtracting $c_0^2\partial^2\rho/\partial x_i^2$ on both sides of the equation yields

$$\frac{\partial^2 \rho'}{\partial t^2}-c_0^2\frac{\partial^2 \rho'}{\partial x_i^2}=\frac{\partial^2 T_{ij}}{\partial x_i \partial x_j}, \tag{10.36}$$

[10] The following equations use the so-called Einstein summation convention: when an index variable appears twice in a single term it implies summation of that term over all the values x, y, z of this index. For example, $\frac{\partial v_i}{\partial x_i}$ means $\frac{\partial v_x}{\partial x}+\frac{\partial v_y}{\partial y}+\frac{\partial v_z}{\partial z}$.

[11] τ_{ij} is defined as [3]:

$$\tau_{ij}=\mu\left[\frac{\partial v_i}{\partial x_j}+\frac{\partial v_j}{\partial x_i}\right]-\frac{2}{3}\mu \text{ div } \boldsymbol{v}.\delta_{ij}$$

As it is, (10.35) is the divergence of the Navier–Stokes equation.

where T_{ij} is the Lighthill tensor:

$$T_{ij} = \rho v_i v_j + (p' - c_0^2 \rho')\delta_{ij} - \tau_{ij} \simeq \rho v_i v_j + (p' - c_0^2 \rho')\delta_{ij}, \tag{10.37}$$

if $p = p_0 + p'$. This last expression is obtained assuming that the forces induced by the fluid viscosity are negligible compared to the convection forces: τ_{ij} can therefore be neglected. This assumption is based on an estimation of the Reynolds number in flute jets, as a ratio between inertial and viscous forces in the flow. In this approach, the equations above describing the basic fluid properties of mass and momentum conservation are subtracted to produce a left-hand term of the equation corresponding to an acoustic wave equation. All the other terms, pushed on the right-hand side are acoustic sources.

This can also be written in terms of the pressure fluctuations p', showing four source terms:

$$\frac{1}{c_0^2}\frac{\partial^2 p'}{\partial t^2} - \Delta p' = \frac{\partial^2 \rho v_i v_j}{\partial x_i \partial x_j} + \frac{\partial^2}{\partial t^2}\left(\frac{p'}{c_0^2} - \rho'\right) + \left[\rho \frac{\partial q_m}{\partial t} - \rho \frac{\partial F_i}{\partial x_i}\right]. \tag{10.38}$$

The first source term is a quadrupole, and corresponds to nonlinear convective terms like vortices and turbulence. The second source term is a monopole and corresponds to entropy fluctuations. The last two terms are not in Eq. (10.36) but have already been discussed for stagnant fluid [see Eq. (1.111)]. They have been added here. The third term is a monopole and corresponds to a mass injection ρq_m, while the last term, dipolar, describes the effect of an external force field density ρF_i acting on the fluid.

An integral formulation of this analogy has been proposed by Curle [13], in order to take the presence of walls with surface S into account, delimiting a volume V.

Sources will be discussed in Chap. 12, but the integral description presented here already introduces this discussion. The acoustic pressure in a given geometry can be written using the Green's function that describes the acoustic response of the system. This function $G(\mathbf{x}, t|\mathbf{y}, \tau)$ corresponds to the acoustic pressure at time t and position $\mathbf{x}$ observed for an impulsive source at time τ and position $\mathbf{y}$. The Green's function is solution of [see, for instance, (4.19)]:

$$\frac{\partial^2 G}{\partial t^2} - c_0^2 \Delta G = \delta(\mathbf{x} - \mathbf{y})\delta(t - \tau). \tag{10.39}$$

Applying this formalism to Lighthill's source terms yields

$$\begin{aligned} p'(\mathbf{x}, t) = &\int_{-\infty}^{t}\int_{V} T_{ij}\frac{\partial^2 G}{\partial y_i \partial y_j} dy d\tau \\ &+ \int_{-\infty}^{t}\int_{S} \rho v_i \frac{\partial G}{\partial \tau} n_i dS d\tau + \int_{-\infty}^{t}\int_{S} \frac{\partial G}{\partial y}(p'\delta_{ij} + \rho v_i v_j) n_j dS d\tau, \end{aligned} \tag{10.40}$$

where V is the volume in which all sources are located, S is the surface bounding volume V, with n_i the outgoing normal. While the last equation is an exact solution that helps to improve our understanding of the sound production mechanisms, it can only be applied to the modeling at the expense of severe simplifications, regarding both the acoustic response of the system (Green's function) and the flow, as illustrated in the following paragraphs.

10.4.3.2 Low Frequency Approximation

At frequencies lower than the pipe cutoff frequency, only plane waves propagate (see Chap. 7) and the Green's function of a 1D infinite pipe can be used

$$G(x_1, t|y_1, \tau) = \frac{c}{2S} H(t^* - \tau), \tag{10.41}$$

where $H(t)$ is the Heaviside step function, the index "1" indicates the pipe direction and $t^* = t - \frac{x_1 - y_1}{c}$ is the retarded time, taking the sound propagation from source to observer into account.[12] Using the symmetry properties of the Green's function $\partial G/\partial x_1 = -\partial G/\partial y_1$, the derivatives of the Green's function $\partial G/\partial y_1 = 1/2\,\mathrm{sgn}(x_1 - y_1)\delta(t^* - \tau)$ and $\partial G/\partial t = -c/2\delta(t^* - \tau)$, and assuming further that the volume is small compared to the acoustic wavelength λ (compact source assumption, $\partial/\partial t << c/\lambda$), the pressure then writes [12]

$$\begin{aligned} p_1'(x_1, t) = &-\frac{c}{2S}\int_S [\rho v_i]_{t^*} n_i dS \\ &- \frac{1}{2S}\,\mathrm{sgn}(x_1 - y_1)\int_S p'(y_1, t^*) n_1 dS - \frac{1}{2S}\,\mathrm{sgn}(x_1 - y_1)\int_S \left[\rho v_1 v_j\right]_{t^*} n_j dS. \end{aligned} \tag{10.42}$$

The first term describes the mass flow going out of the source volume V, while the second term describes the pressure forces acting on the surface bounding the source volume, and the third term corresponds to nonlinear convective contributions in the flow (turbulence and vortices).

In the application to sound production in flutes, if the total jet volume flow is assumed to be constant (see Sect. 10.5.2 for a discussion on this topic), the first term does not produce any sound. Furthermore, for values of the Reynolds number less than a few hundreds, the sound produced by turbulence is negligible. The main source terms then lie in the pressure term and in the vortices.

A similar analysis developed by Powell [34] in the case of edge-tones, i.e., a jet flowing towards a labium without acoustic resonator, shows that the dominant term is the unsteady force exerted by the flow on the labium. This force corresponds to

[12] It is in fact the first term of (4.20) and (4.21), since the infinite pipe does not show any reflection.

the stagnation pressure of the jet and the amplitude of the oscillating force is (H is the width of the jet in the transverse direction):

$$F_a = \frac{1}{2}\rho H \int U(y)^2 dy, \tag{10.43}$$

which has been confirmed by experiments [40].

Finally, in the case of edge-tones, the source term can be written in terms of a dipole, such as the one written in Sect. 10.4.1, provided that the potential distance δ_d between source and sink is a function of the jet velocity, or of the hydrodynamic wavelength $\lambda_h = 2\pi c_p/\omega$ of the perturbations on the jet:

$$\delta_d \approx \lambda_h/2. \tag{10.44}$$

Both approaches, the aeroacoustic and the more acoustically intuitive presented in Sect. 10.4.1 are in line, provided that the source-sink distance in the jet-drive model corresponds to half the hydrodynamic wavelength, and therefore depends on the jet velocity and on the frequency.

10.4.3.3 Increasing the Jet Velocity

The analysis presented above is restricted to relatively low Reynolds numbers and low frequencies. When the jet velocity is increased, sound production by turbulence becomes more and more important. Verge [44] presented a study of sound production by turbulence of a jet impinging on a labium in an infinite pipe, assuming no synchronized jet oscillations. The two first terms in Eq. (10.42) vanish and the pressure is written as:

$$p'(x_1, t) = -\frac{1}{2S}\,\mathrm{sgn}(x_1 - y_1) \int_S \rho v_{1_{t^*}}^2 dS, \tag{10.45}$$

showing that the acoustic power ranges as the fourth power of the jet velocity or of the Mach number $M = U_0/c$:

$$P_{\mathrm{ac}} \propto M^4. \tag{10.46}$$

In a sound synthesis by physical modeling, adding to the source terms a broadband noise that follows this power law improves the realism of the synthesis. This shows how important the turbulence noise is for the perception of the sound identity of flutes.

10.4.3.4 Vortex Shedding at the Labium

In a theoretical analysis of the problem, Howe [28] proposes a model for the sound production in flutes based on the vortex sound theory. The sound production is due to the action of the Coriolis force on the acoustic field [see Eq. (10.33)]. In this model, the sound is generated at each period by a vortex shed at the labium, triggered by the flow induced by the acoustic resonance in the pipe. This vortex is then convected by the jet (see Fig. 10.23). In this framework, the sound production in a flute has been estimated, based on flow visualizations that show the exact phase of the triggering of this vortex. It appears that, due to the phase relation between the different terms, the sound production is negative [21]: the vortex does not produce sound as was assumed by Howe [28] but rather absorbs acoustic energy. Furthermore, the analysis of the different losses, under standard blowing conditions in a recorder, indicates that the losses induced by the vortex shedding at the labium is one of the dominant mechanism that limits the oscillation amplitude.

The vortex sound theory of Howe is also interesting for thick jet configurations. The vorticity in the jet shear layers is represented as discrete vortices, triggered by the acoustic perturbation. These vortices are convected at a constant velocity of approximately half the main flow velocity, with a circulation that grows linearly with time.[13] Notice that the vortices considered here are not those shed at the labium like in Howe's model [28], but those formed at the flue exit, corresponding to the jet shear layers. The model proposed by Meissner for a whistle is built with this description. It seems to give an accurate prediction of the oscillating frequency

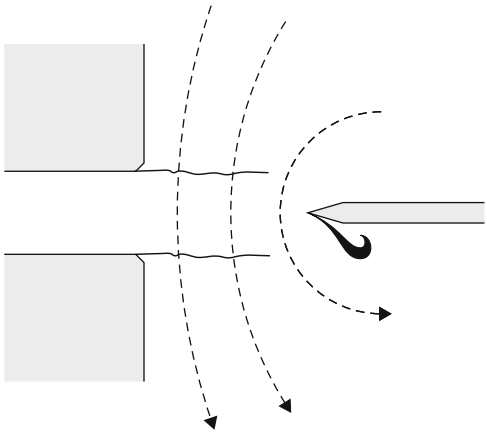

Fig. 10.23 Vortex shedding at the labium, due to the separation of the flow induced by the acoustic field. *Dashed lines* indicate streamlines of the potential flow associated with the acoustic velocity

[13] See, for example, the work by Meissner [32] in the case of a whistle and Dequand [15], inspired by Nelson's [24, 33] and Holger's [27] descriptions. A difference between the two models is that Dequand assumes that the circulation of each vortex grows during one oscillating period only, while Meissner assumes that the circulation grows without saturation, but only takes the vortices between the flue exit and the labium into account.

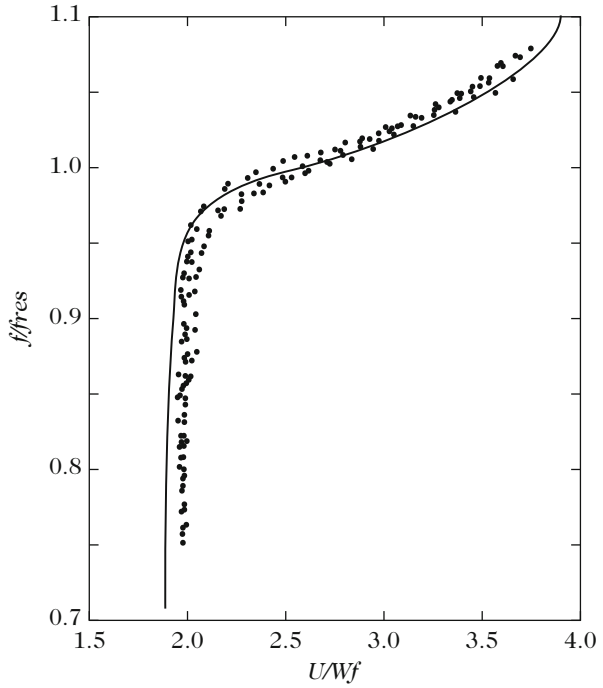

Fig. 10.24 Dimensionless frequency f/f_{res} of the oscillation in a Helmholtz resonator (f_{res} is the passive resonance frequency) as function of the dimensionless jet velocity (or inverse Strouhal number) $\text{Str}^{-1} = U/Wf$, U is the jet velocity, W is the flue exit to labium distance. For low jet velocities, the oscillation appears at frequency lower than the resonance frequency. It corresponds to a constant Strouhal number, indicating that the frequency is proportional to the jet velocity. After [32]

(Fig. 10.24) but not of the amplitude. This indicates that even if phase terms are well described in the model, losses are still difficult to estimate.

The oscillating frequency in flutes and organ pipes on the first regime shows a double slope behavior:

- for low jet velocities and oscillation at frequency lower than the pipe resonance, the oscillation appears to be at constant Strouhal number, that is at frequency proportional to the jet velocity.
- For higher jet velocities, the frequency grows much slower, due to the strong phase rotation with frequency of the acoustic response of the pipe, as shown by Auvray [2].

The frequency behavior at low jet velocities is responsible for the so-called mouth-tones observed in some organ pipes [19], during attack transients, or for low blowing conditions [8]. Notice that these mouth-tones are quite different from edge-tones, since they rely on the pipe resonance: Auvray showed that they are accurately

predicted using a model considering only the feedback of the pipe, while edge-tones rely on a direct hydrodynamic feedback [27], because there is no pipe in the edge-tone configuration.

10.5 A Lumped Model of the Oscillation in a Flute

A simplified description of the self-sustained oscillation in the flute has been presented in Sect. 10.1.1. This description can now be improved by including the aspects presented in the previous sections. In order to achieve this, we first need to describe complementary aspects:

- nonlinear losses at the window;
- jet velocity fluctuations;
- direct hydrodynamic feedback of the sources on the jet.

These three points are developed in the following section to be later integrated in lumped description of the self-sustained oscillator.

10.5.1 Nonlinear Losses at the Blowing Window

The blowing window is an open end of the pipe. The area of this window is smaller than the main pipe cross section, resulting in an increased acoustic velocity as compared to the other pipe end. Under standard blowing conditions, the acoustic velocity in the blowing window is about one-tenth of the jet velocity. The labium edge is generally sharp, at least sharper than the other edges in the instrument, and a nonlinear behavior of the flow induced by the acoustic resonance is expected: velocities are high enough to trigger flow separation at the edge of the labium, as a consequence of viscosity. Several models can be used to describe the losses induced by this flow separation [21]. We will focus on the most simple one, inspired from [30] (see also Chap. 8, Sect. 8.4.5). If we first assume an inviscid 2D incompressible flow, the flow can be described as a potential flow (see Fig. 10.25 left) and the fluid acceleration in the window is associated with a pressure decrease. After the window, the fluid slows down and the pressure rises to its initial value. Notice that, when passing close to the labium edge, the fluid is submitted to strong accelerations: a sharp edge induces a singularity in a potential flow.

If we no longer assume the flow to be inviscid, viscosity induces the flow separation, resulting in a jet formation (see Fig. 10.25 right). The initial pressure drop induced by the flow acceleration is no longer compensated: flow separation can be modeled as a pressure difference between the two sides of the labium:

$$\Delta p_{\text{sep}} = p_p - p_m = -\frac{1}{2}\rho \left(\frac{v_{\text{ac}}}{\alpha_v}\right)^2 \text{sgn}(v_{\text{ac}}), \tag{10.47}$$

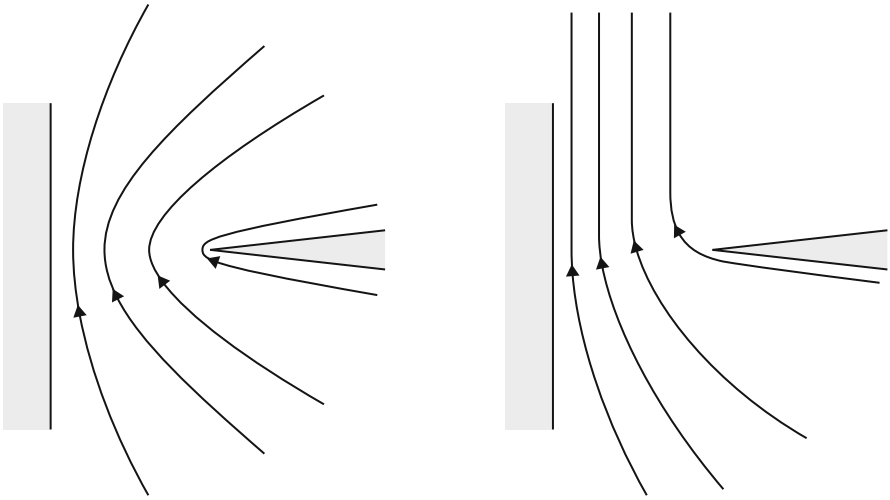

Fig. 10.25 Influence of viscosity on the flow induced by the acoustic resonance : without viscosity (*left*), the flow is potential and strong acceleration appear near the tip of the labium. Viscosity (*right*) is responsible for the flow separation and jet formation

where α_v corresponds to the *vena contracta*[14] with values $\alpha_v \approx 0.6$; v_{ac} is the acoustic velocity in the window, oriented towards the inside, while p_p and p_m are the pressures on both sides of the window. The pressure difference changes in sign with the acoustic velocity in the window, and depends on the square of the oscillating amplitude. It is therefore a dominant mechanism in the amplitude saturation of the oscillation in steady oscillation [21]. This was first observed and described in terms of a nonlinear "impedance" by Coltman [9]. It is the reason why the dimensionless oscillating amplitude does not depend on the frequency [47] (see Fig. 10.26): indeed, viscous, thermal, and radiation losses are frequency dependent and the oscillating amplitude would be frequency dependent if they were dominant!

This mechanism is the same as the one discussed in Sect. 10.4.3 of the present chapter, and also in Chap. 8 (Sect. 8.4.5).

10.5.2 Jet Velocities Fluctuations

All models presented above assume that the jet velocity is constant. The jet flow has been shown to be induced by the pressure in the player's mouth, accelerating the

[14]Inertia of the fluid particles induces flow separation in the direction given by the wall from which the flow separates. This results in a jet with a smaller width than the actual size of the window, smaller by a factor α_v.

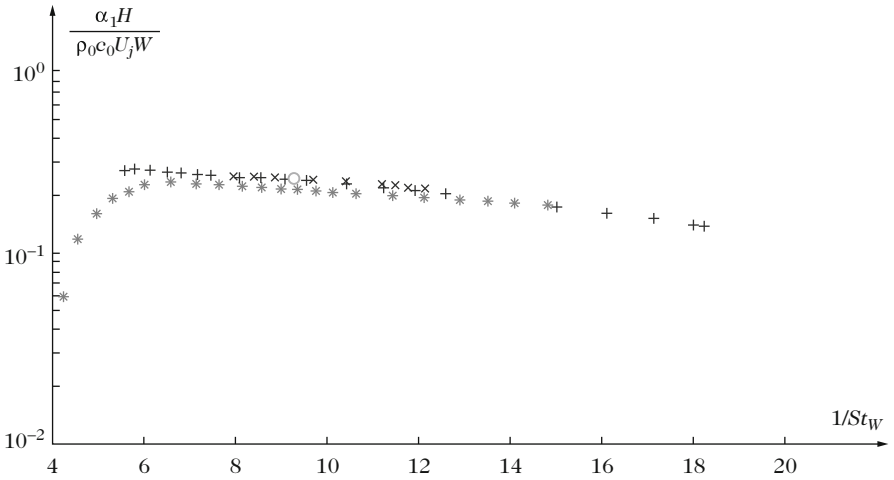

Fig. 10.26 The oscillating amplitude in a small organ pipe (square cross section (2 cm × 2 cm), 28 cm length and $W = 4$ mm flue exit to labium distance) is here presented in a dimensionless form for the four first oscillating regimes, corresponding to the four first pipe resonances: *asterisk symbol*, 1st, *plus symbol*, 2nd, *cross symbol*, 3rd, *open circle*, 4th. The amplitude of the fundamental is made dimensionless as the ratio of the acoustic velocity in the blowing window to the jet velocity, plotted as function of the dimensionless jet velocity U_j/fW. After [47]

flow into the channel. But, until now, we did not take the pressure fluctuations at the flue exit into account, due to the pipe resonance, added to the mean (atmospheric) pressure. Indeed, the flue exit is close to the open end of the pipe, but acoustic pressure at this position can still be around 60 % of the mode amplitude, depending on the end correction [10].

For a flue channel of length L, the jet velocity U_j can be estimated using the unsteady Bernoulli equation:

$$\rho l_c \frac{dU_j}{dt} + \frac{1}{2}\rho U_j^2 = p_{\text{res}} - p_{\text{exit}}, \tag{10.48}$$

where p_{res} is the reservoir pressure in the player's mouth and p_{exit} is the pressure at the channel exit.

The average jet velocity can be approximated as $\langle U_j \rangle = \sqrt{2p_{\text{res}}/\rho}$ and the total jet velocity is $U_j = \langle U_j \rangle + U_j'$. Because of the jet velocity fluctuations, the reservoir pressure can also fluctuate around its average value $p_{\text{res}} = \langle p_{\text{res}} \rangle + p'_{\text{res}}$, and the jet velocity fluctuations at the fundamental frequency ω of the oscillation can be written as:

$$U_j' \approx \frac{p'_{\text{res}} - p_{\text{exit}}}{\rho(j\omega L + \langle U_j \rangle)}. \tag{10.49}$$

For a short channel, jet velocity fluctuations are in opposite phase with the acoustic pressure at the flue exit: the instantaneous velocity increases when the pressure decreases. The acoustic work performed is therefore negative, and the jet velocity fluctuations act as losses. Air inertia in the channel becomes important when the channel is longer, and $\rho j\omega L$ becomes more important: jet velocity fluctuations are reduced and the phase shift relative to the acoustic pressure increases. A simple description can be used to describe the jet velocity fluctuations, by adding a volume flow source term $Q'_j = S_{\text{lum}} U'_j$ at the end of the resonator. In a more developed description, the jet velocity fluctuations can be integrated directly in the source mechanism as proposed by Auvray [2] with interesting influence on the balance between odd and even harmonics that affect the timbre.

Jet velocity fluctuations can be modulated by the player, adjusting mouth resonances: the jet velocity fluctuations are responsible for acoustic pressure in the mouth cavity, and the player has therefore control on the jet fluctuations. According to players, this is an important element of the control of the tone quality.

Pressure signals recorded in the foot of a small organ pipe and in the pipe, close to the labium, are presented in Fig. 10.27.

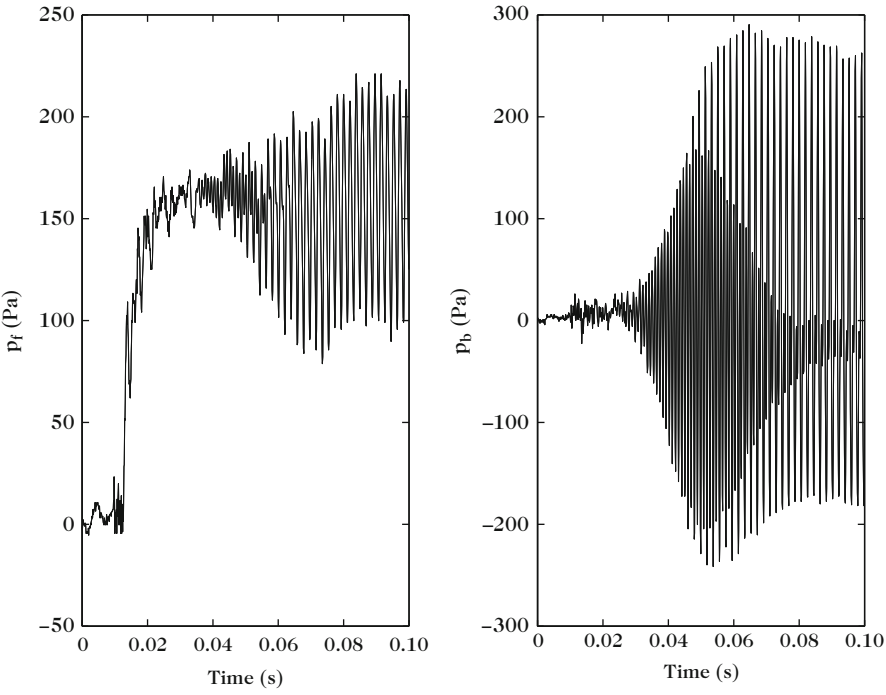

Fig. 10.27 Pressure signal in the foot (P_f) and close to the labium P_b of a small organ pipe. Strong pressure fluctuations appear in the foot, induced by the acoustic pressure in the pipe. Please note that the mean pressure in the foot and the amplitude of the acoustic pressure in the pipe are of the same order of magnitude. The pressure drop between foot and flue exit shows fluctuations that may become larger than the mean pressure: the jet velocity fluctuates around its mean value. After [47]

10.5.3 Direct Hydrodynamic Feedback

Aeroacoustic sources associated with the jet oscillation have been presented as two volume flow injections with opposite phases. While this source sustains the acoustic oscillation in the pipe, it also induces a local velocity field, that may contribute to the jet perturbation. This is a hydrodynamic direct feedback, which controls the oscillation in edge-tones. For self-sustained oscillation under normal playing conditions in a flute, this hydrodynamic feedback is negligible during steady-state oscillation, compared to the feedback from the resonator (about 4 % of the perturbation coming from the resonator [45]).

10.5.4 The Minimal Oscillator

All the different elements can be lumped to build a simple model for self-sustained oscillations in a flute, as presented in Fig. 10.4. Basic hypothesis for the model of the excitation are

- a constant jet velocity U_j, as estimated following Bernoulli (10.7),
- an exponential growth of the jet transverse displacement, independent of frequency,
- a convection velocity of perturbations on the jet, estimated as $c_p \approx 0.4U_j$,
- a dipole source associated to the jet oscillation at the labium.

The model is then described by the following equations:

- the jet transverse displacement at the labium is written as:

$$\eta(W,t) = \frac{h}{U_j} v_{\text{ac}}(t - W/c_p) e^{\alpha_i W}; \tag{10.50}$$

  where α_i comes from the resolution of Rayleigh's equation (10.21).
- the aeroacoustic source at the labium acts as a pressure step:

$$\Delta p_{\text{dip}} = -\frac{\rho \delta_d}{S_m} \frac{dQ_1}{dt}; \tag{10.51}$$

  where Q_1 is the part of the jet volume flow passing under the labium:

$$Q_1 = H \int_{y_0}^{\infty} U(y - \eta) dy, \tag{10.52}$$

where y_0 is the transverse position of the labium, relative to the jet and channel symmetry axis, and H is the jet width. For smooth velocity profiles induced by viscous spreading of the jet, the volume flow Q_1 is a smoothly nonlinear function, as for instance $U_0 H \tanh(2y/h)$. The main difference between flute models and models for simple reed instruments is the delay induced by convection of perturbations on the jet.

- losses induced by flow separation of the labium:

$$\Delta p_{\text{sep}} = -\frac{1}{2}\rho \left(\frac{v_{\text{ac}}}{0.6}\right)^2 \text{sgn}(v_{\text{ac}}). \tag{10.53}$$

This nonlinear loss term is very important for the saturation of the oscillating amplitude, but is not necessary during the starting transient of the oscillation. Please note that this pressure difference, as the one in (10.51), is a pressure step between the inside and the outside of the blowing window $\Delta p = p_p - p_m$.

- the acoustic response of the pipe is build in the frequency domain, using a low frequency 1D approximation (see Fig. 10.21). The source is introduced using mass conservation in the blowing window $Q_m = S_m v_{\text{ac}} = Q_p$ and adding the two pressure steps (dipolar source and losses). The acoustic response of the pipe is then[15]:

$$Q_m = \frac{\Delta p_{\text{tot}}}{Z_m + Z_p}, \tag{10.54}$$

where Z_m and Z_p are the acoustic impedances of the blowing window (to a first approximation, this is a mass, equivalent to a length correction) and of the resonator (input impedance).[16]

All the different elements are lumped as shown in Fig. 10.28. Time domain simulation of the equations of the model has been proposed by several authors (for instance, [14, 44]), allowing sound synthesis by physical modeling. The sound quality and realism of the synthesis is greatly enhanced by adding a wideband noise scaling with the jet velocity to the source terms, in order to model the turbulence. Some other aspects presented in the previous sections can also be integrated in order to provide a more complex model. This allows to take some important aspects for instrument makers into account, such as the channel shape and the chamfers at the flue exit.

[15]The same development is presented in Eq. (7.63) in Chap. 7, where the flow rate is written as U instead of Q.

[16]Please remind that impedances are defined as passive systems, that is with positive real part (see Sect. 1.3.3.1 in Chap. 1). We therefore have: $Q_m = -Z_m p_m$ and $Q_p = Z_p p_p$.

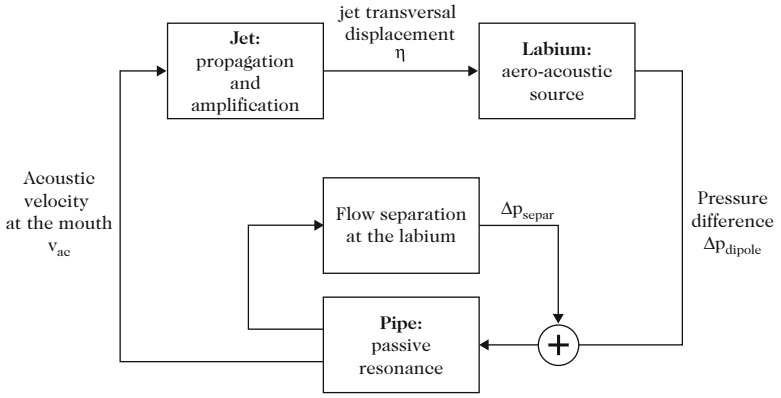

Fig. 10.28 Simplified model for self-sustained oscillations in a flute-like instrument. The nonlinear element that initiates the sound production is the saturation of the source at the labium, the other nonlinear element modeling the flow separation at the labium is essential for saturating the oscillation at a reasonable amplitude

10.6 Discussion About the Model

Different approaches to describe the elements of a model were presented in the previous sections. Each approach has its own limitations and ranges of validity, that would be interesting to point out, together with common ranges and transitions between models. A summary is presented below with regard to the sources, the instability and the receptivity.

- The *sources* can be described, to a first approximation, as a pressure step with an amplitude depending on the exact position of the flow injection points, or rather on the equivalent distance between them. Several clues indicate that this position may vary with the hydrodynamic wavelength on the jet. This wavelength does not vary much under standard blowing conditions of the instrument, and therefore, a fixed position of the injection points is fair as a first approximation. This model is restricted to low values of the Strouhal number, for which the jet does not break down into discrete vortices, typically $\mathrm{Str} = Wf/U_j < 0.3$ [15]. The amplitude of the pressure source Δp can be deduced from the transverse jet displacement η at the labium. For displacement larger than the jet thickness, Δp is a saturated function of the displacement η. When the displacement η is smaller or similar to the jet thickness, the integration of the jet velocity profile is necessary to calculate the pressure source Δp from the jet displacement η. It can be linearized for small amplitudes.

  For small amplitudes of the jet transverse displacement, in the case of a short distance W from flue exit to labium, for example, the instability does not have space to develop enough. In such a case, a better candidate is the model of Dequand [15], following [29, 33], in which the aeroacoustic source is the Coriolis

force due to the vortices that model the shear layer. This corresponds to "thick" jets, with values of W/h smaller than 2 [15]. This kind of model can also apply to thin jets ($W/h > 5$ typically) with high values of the Strouhal number, where the jet breaks into discrete vortices [26].

Finally, for turbulent jets and low values of the Strouhal number (or thick jets), the model by Howe [28] of sound production by vortices shed at the labium should still be evaluated. Even for values of the Reynolds number smaller than 2500, turbulence can significantly affect the behavior of the instrument, at least through the broadband noise generated. The first transverse acoustic resonance of the pipe seems to be strongly coupled to turbulent sources. This affects the sound quality of instruments with large bores like the bass flute of some organ pipe stops.

- The *instability* of the jet can be studied, in the case of laminar jets, through three different approaches: using a linear theory (Rayleigh), using discrete vortices to describe each shear layer of the jet, or using an alternate vortex street (Holger [26]).

  The linear model, inspired by Rayleigh, is well adapted to thin jets, with less than a half hydrodynamic wavelength between flue exit and labium. This corresponds to low values of the Strouhal number. When this condition is not fulfilled, a better candidate is Holger's model, which turns the thin jet into an alternate vortex street. In the case of very thick jets, the model of Dequand should be used since it better describes the vorticity in each shear layer. It is interesting to recall that Holger's model assumes an initial linear growth of vorticity in the shear layers before the jet breaks into a vortex street.

  For turbulent jets, the work of Bechert [4] is an interesting direction. Turbulence is not fully developed, and the study of the triggering of the turbulence, including geometrical aspects of the reservoir, would be very interesting.
- Receptivity still remains a very difficult problem. Flute makers and players as well as experiments [7, 40] on this subject indicate that the geometry of the flue exit strongly influences the receptivity. The work by Blanc [7] suggests that the chamfers in a recorder control both a protection effect due to the standing back of the flow separation points and a relative orientation of the perturbative acoustic velocity compared to the jet flow. This work should be continued in the future.
- In this chapter, the analysis focused on open pipe flutes. Closed pipe instruments have special sounding qualities, mostly because of the spectral content of the sound they produce, dominated by odd harmonics: closed organ pipes, Pan flutes... From the physical point of view, some specificities should be included in the model. First, these instruments are most often played with a turbulent jet. Second, the closed end of the pipe induces a recirculation of the air flow. As a consequence, the jet, submitted to a cross flow, bends towards the outside of the pipe.

References

1. Artaud, P., Geay, G.: Present Day Flutes (in French). Ed Jobert/Transatlantiques, Paris (1980)
2. Auvray, R., Fabre, B., Lagrée, P.: Regime change and oscillation thresholds in recorder-like instruments. J. Acoust. Soc. Am. **131**(2), 1574–1585 (2012)
3. Batchelor, G.: An Introduction to Fluid Dynamics. Cambridge University Press, Cambridge (1976)
4. Bechert, D.: The control of a plane turbulent free jet by a lateral flow generated in a sound field (in German). Z. Flugwiss. **24**, 25–33 (1976)
5. Bechert, D.: Excitation of instability waves in free shear layers part I. Theory. J. Fluid Mech. **186**, 47–62 (1988)
6. Blake, W.K.: Mechanics of Flow Induced Sound and Vibration. Academic, London (1986)
7. Blanc, F., Francois, V., Fabre, B., de la Cuadra, P., Lagrée, P.: Modeling the receptivity of an air jet to transverse acoustic disturbance with application to musical instruments. J. Acoust. Soc. Am. **135**, 3221–3230 (2014)
8. Castellengo, M.: Acoustical analysis of initial transients in flute like instruments. Acustica Acta Acustica **85**, 387–400 (1999)
9. Coltman, J.: Sounding mechanism of the flute and organ pipe. J. Acoust. Soc. Am. **44**, 983–992 (1968)
10. Coltman, J.W.: Jet drive mechanisms in edge tones and organ pipes. J. Acoust. Soc. Am. **60**(3), 725–733 (1976)
11. Crighton, D.: The edgetone feedback cycle. Linear theory for the operating stages. J. Fluid Mech. **234**, 361–391 (1992)
12. Crighton, D.: Nonlinear acoustics. In: Modern Methods in Analytical Acoustics (Lecture Notes). Springer, London (1992)
13. Curle, N.: The influence of solid boundaries upon aerodynamic sound. Proc. R. Soc. Ser. A **231**, 505–514 (1955)
14. De la Cuadra, P.: The sound of oscillating air jets: physics, modeling and simulation in flute-like instruments. Ph.D. thesis, Stanford University (2005)
15. Dequand, S.: Simplified models of flue instruments: influence of mouth geometry on the sound source. J. Acoust. Soc. Am. **113**(3), 1724–1735 (2003)
16. Drazin, P.: Introduction to Hydrodynamic Stability. Cambridge University Press, Cambridge (2002)
17. Elder, S.: The mechanism of sound production in organ pipes and cavity resonators. J. Acoust. Soc. Jpn. (E) **13**(1), 11–23 (1992)
18. Fabre, B.: Sound production in flute-like instruments: aeroacoustic modeling and time domain simulation (in French). Ph.D. thesis, Université du Maine, le Mans (1992)
19. Fabre, B., Castellengo, M.: Transients in flue organ pipes: experiments and modeling. In: Proceedings of the 17th ICA, Roma (2001)
20. Fabre, B., Hirschberg, A., Wijands, A., van Steenbergen, A.: Attack transients in flute-like instruments (in French). In: de Physique, L.E. (ed.) 2ème Congrès Français d'Acoustique, vol. C1, pp. 67–70 (1992)
21. Fabre, B., Hirschberg, A., Wijnands, A.: Vortex shedding in steady oscillation of a flue organ pipe. Acustica Acta Acustica **82**, 811–823 (1996)
22. Fletcher, N.H., Rossing, T.D.: The Physics of Musical Instruments. Springer, New York (1991)
23. Goldstein, M.: Aeroacoustics. McGraw-Hill, New York (1976)
24. Hirschberg, A.: Aero-acoustics of wind instruments. In: Mechanics of Musical Instruments, pp. 291–369. CISM Courses and Lectures, vol. 355. Springer, New York (1995)
25. Hirschberg, A., Rienstra, S.: An Introduction to Aeroacoustics. Eindhoven University of Technology, The Netherlands (2004)
26. Holger, D., Wilson, T., Beavers, G.: Fluid mechanics of the edge-tone. J. Acoust. Soc. Am. **62**, 1116–1128 (1977)

27. Holger, D., Wilson, T., Beavers, G.: The amplitude of edge-tone sound. J. Acoust. Soc. Am. **67**, 1507–1511 (1980)
28. Howe, M.: Contributions to the theory of aerodynamic sound, with applications to excess jet noise and the theory of the flute. J. Fluid Mech. **71**, 625–673 (1975)
29. Howe, M.: Acoustics of Fluid Structures Interactions. Cambridge University Press, Cambridge (1998)
30. Ingard, U., Ising, H.: Acoustic nonlinearity of an orifice. J. Acoust. Soc. Am. **42**, 6–17 (1967)
31. Kühnelt, H.: Vortex sound in recorder- and flute-like instruments: Numerical simulation and analysis. In: International Symposium on Musical Acoustics, pp. Paper 1–S1–6, Barcelona (2007)
32. Meissner, M.: Aerodynamically excited acoustic oscillations in cavity resonator exposed to an air jet. Acustica Acta Acustica **88**, 387–400 (2002)
33. Nelson, P., Halbiwell, N., Doak, P.: Fluid dynamics of flow excited resonance Part 2: theory. J. Sound Vib. **91**, 375–402 (1983)
34. Powell, A.: On the edgetone. J. Acoust. Soc. Am. **33**(4), 395–406 (1961)
35. Prandtl, L., Tietjens, O.: Fundamentals of Hydro and Aeromechanics. Dover, New York (1934)
36. Rayleigh, L.: The Theory of Sound, vol. 2. Dover, New York (1877). Second edition, 1945 re-issue
37. Rienstra, S., Hirschberg, A.: An Introduction to Acoustics. Eindhoven University of Technology, Eindhoven (2006)
38. Ségoufin, C.: Sound production by flow/acoustical resonator interaction: influence of the upstream system - application to the recorder (in French). Ph.D. thesis, University Paris 6 (2000)
39. Segoufin, C., Fabre, B., Verge, M., Hirschberg, A., Wijnands, A.: Experimental study of the influence of the mouth geometry on sound production in a recorder-like instrument: windway length and chamfers. Acustica Acta Acustica **86**, 599–610 (2000)
40. Ségoufin, C., Fabre, B., de Lacombe, L.: Experimental investigation of the flue channel geometry influence on edge-tone oscillations. Acustica Acta Acustica **90**(5), 966–975 (2004)
41. Skordos, P.A.: Modeling flue pipes: subsonic flow, lattice Boltzmann, and parallel distributed computers. Ph.D. thesis, Massachusetts Institute of Technology, Cambridge (1995)
42. Tritton, D.: Physical Fluid Dynamics, 2nd edn. Oxford University Press, Oxford (1995)
43. van Zon, J., Hirschberg, A., Gilbert, J., Wijnands, A.: Flow through the reed channel of a single reed music instrument. J. Phys. IV Colloques **51**(C2), 821–824 (1990)
44. Verge, M.P.: Aeroacoustics of confined jets, with application to the physical modeling of recorder-like instruments. Ph.D. thesis, TU Eindhoven (1995)
45. Verge, M., Caussé, R., Fabre, B., Hirschberg, A., Wijnands, A., van Steenbergen, A.: Jet oscillations and jet drive recorder-like instruments. Acustica Acta Acustica **2**, 403–419 (1994)
46. Verge, M., Fabre, B., Mahu, W., Hirschberg, A., van Hassel, R., Wijnands, A., de Vries, J., Hogendoor, C.: Jet formation and jet velocity fluctuations in a flue organ pipe. J. Acoust. Soc. Am. **95**, 1119–1132 (1994)
47. Verge, M., Fabre, B., Hirschberg, A., Wijnands, A.: Sound production in recorder-like instrument I. Dimensionless amplitude of the internal acoustic field. J. Acoust. Soc. Am. **101**, 2914–2924 (1997)
48. Von Helmholtz, H.: On the Sensation of Tones (orig. "Lehre von den Tonempfindungen", 1862). Engl. translation: Dover, New York (1954) (1877)